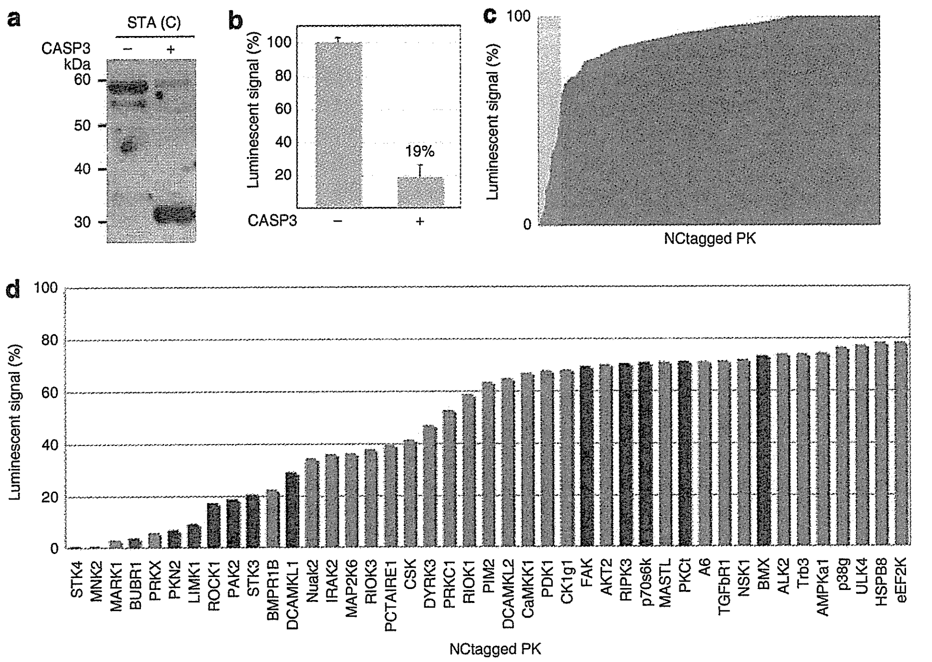

Figure 2 Screening of CASP3-cleaved PK substrates from the NCtagged PK library. (**a**) Immunoblot of NCtagged PAK2 that had been incubated in the presence (+) or absence (−) of CASP3. Alexa488-labeled streptavidin (STA(C)) was used for detection. (**b**) Detection of CASP3-cleaved NCtagged PAK2 using the AlphaScreen system. The luminescence for the control (no CASP3) was set to 100%. The value of 19% indicated that most of the NCtagged PAK2 was cleaved by CASP3. Each value is the mean of three independent experiments, and the uncertainty is reported as the standard deviation. (**c**) Luminescent signals remaining after *in vitro* CASP3 treatment of NCtagged PKs that had been synthesized in the wheat cell-free system. The *x* axis lists the NCtagged PKs in ascending order of their luminescent signals after CASP3 treatment. (**d**) NCtagged PKs that returned luminescent signals of <78% of the control values. The plot contains the data of (**c**) within the green rectangle. Red bars are for PKs that were known to be substrates of CASP3 before this report

using this system. CASP3 treatment decreased the luminescent signal to 19±7% that of the control (no CASP3; Figure 2b). Therefore, the system could detect CASP3 cleavage and can replace conventional immunoblotting procedures.

Screening of the CASP3-substrate kinome. Using the luminescent system, 304 NCtagged PKs were screened. The level of luminescence after CASP3 treatment is reported as the percentage of the corresponding control (no CASP3; Figure 2c and d). Thirteen of the NCtagged PKs for which luminescence was low after CASP3 treatment are known CASP3 substrates.[23,24,26] The smallest and largest luminescent values were for STK4 (1%) and BMX (73%), respectively; we therefore examined the physical states of the PKs that had been treated with CASP3 and had associated luminescence values of ~80% by immunoblotting with anti-Flag antibodies and Alexa488-streptavidin to detect the N- and C-termini of the NCtagged PKs, respectively. This 'terminal detection' (TD) immunoblot assay identified 43 NCtagged PKs that had been cleaved (Supplementary Table S1). In addition to the 13 PKs that were known to be CASP3 substrates, 30 previously unidentified PK that were substrates of CASP3 were found (Figure 3 and Table 1). In addition, because the apparent molecular weights of the N- and C-terminal fragments could be estimated from their positions in the TD immunoblot, the CASP3 cleavage sites could be predicted (red arrowheads, Figure 3). For MASTL, the signal on the immunoblot with Alexa488-conjugated streptavidin was not detectable, probably indicating that the efficiency of biotinylation in MASTL proteins might be too low to detect for the immunoblot. Luminescent signal of this clone was also very low (see Supplementary Table S1).

A comparison of the luminescent and immunoblot data correlated a luminescent signal of <78% with a positive immunoblot result. Forty-eight PK constructs with luminescent signals >78% were tested and returned negative immunoblot results (Supplementary Table S1). Therefore, a luminescent signal of ~78% is the apparent divisor between PKs that can be cleaved by CASP3 and those that cannot be cleaved.

***In vivo* identification of the PKs that were identified as CASP3 substrates by the luminescent assay.** We investigated whether the newly identified PKs that were substrates of CASP3 were cleaved in HeLa cells that had been induced to undergo apoptosis by TNFα plus cycloheximide (TNFα)[27] or anti-Fas antibody (anti-Fas).[28] The genes encoding these PKs were each inserted into the transfection vector, pDEST26, using the Gateway system and expressed as $(His)_6$-PK-Flag constructs. We were able to detect all expressed PK constructs, except DYRK3, by immunoblotting with anti-$(His)_6$ or anti-Flag antibodies.

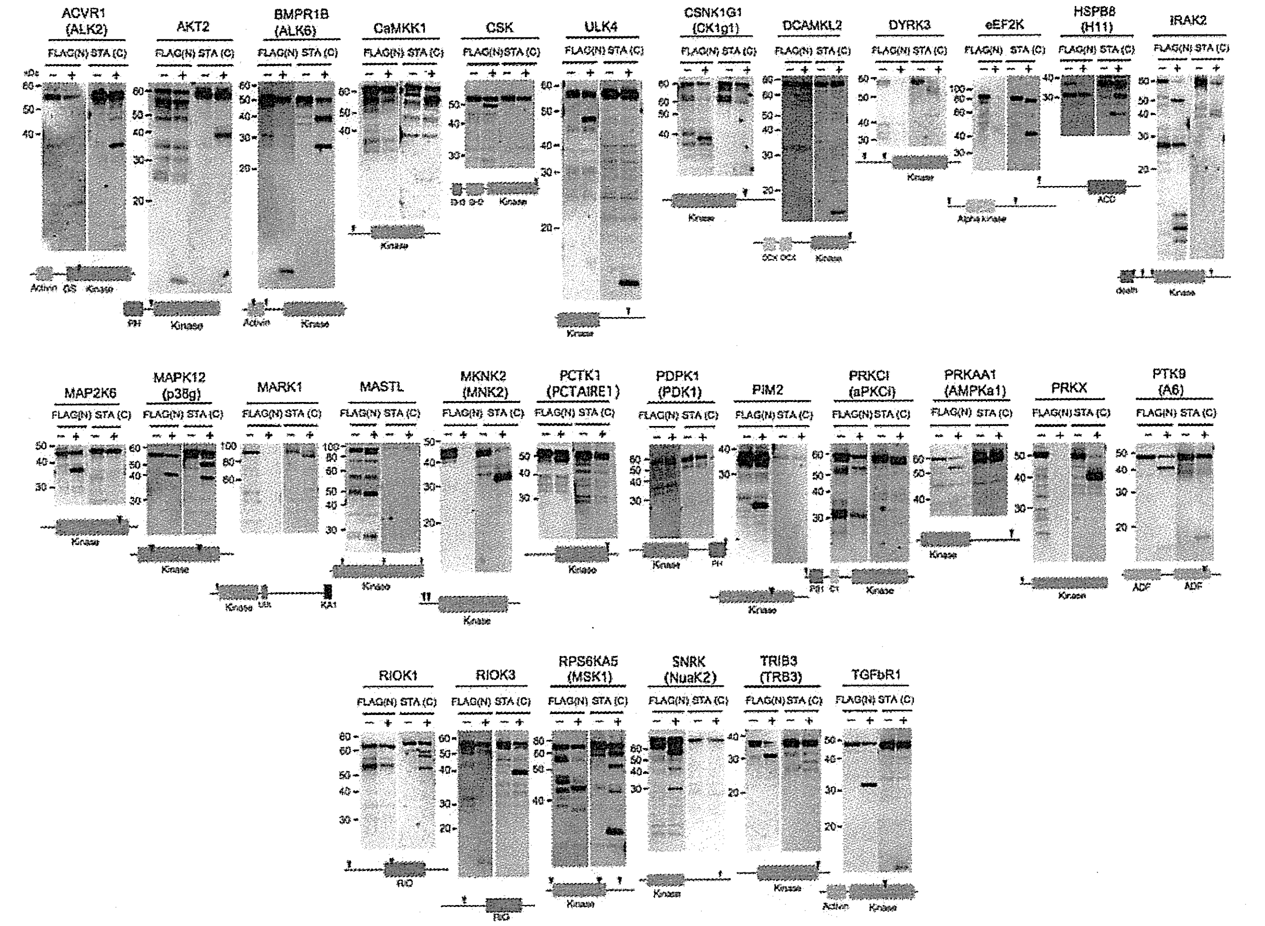

Figure 3 *In vitro* cleavage of NCtagged PKs by CASP3. The NCtagged PKs that had been incubated in the presence (+) or absence (−) of CASP3 and their cleavage products were detected using anti-Flag antibodies (FLAG(N)) and Alexa488-conjugated streptavidin (STA(C)), which bound to the N- and C-termini of the PK constructs, respectively. The cartoons of the proteins that are under the lanes show the locations of the conserved domains (colored boxes) and the predicted cleavage sites (red arrowheads). The conserved domains that are found in the Conserved Domains Database (http://www.ncbi.nlm.nih.gov/cdd) are: ACD, alpha-crystallin domain; activin, conserved domain for activin members; ADF, actin depolymerization factor/cofilin-like domain; α-kinase, conserved kinase domain for the α-kinase family; C1, phorbol esters/diacylglycerol binding domain; DCX, doublecortin domain; death, death domain; GS, GS motif; KA1, kinase-associated domain; kinase, catalytic domain of protein kinase; PB1, Phox and Bem1p domain; PH, pleckstrin homology domain; RIO, catalytic domain of eukaryotic RIO kinase family; SH2, src homology 2 domain; SH3, src homology 3 domain; UBL, ubiquitin-like domain

Notably, they were detected as cleavage products and/or were found in smaller amounts when the cells had been induced to undergo apoptosis than when apoptosis had been inhibited by z-VAD-FMK (Figure 4a and b). Furthermore, apoptosis-induced cleavage of four endogenous PKs was found by immunoblotting with commercially available antibodies against the endogenous PKs (Figure 4c). These *in vivo* experiments validated the underlying concept of our *in vitro* cell-free system as the *in vivo* system found all of the PKs identified by the *in vitro* system.

Characterization of the CASP3 cleavage sites in the newly identified PK substrates. We characterized the CASP3 cleavage sites in the newly identified PK substrates. As the positions of the cleaved PK fragments in the TD immunoblot could be used to estimate the size of the cleaved fragments and because the antibodies could be used to identify whether the fragments were derived from the N- or C-terminal regions of the PKs, we could predict the approximate positions of the CASP3 cleavage sites (red arrowheads, Figure 3). Each NCtagged PK that was a substrate for CASP3 was synthesized in the cell-free system and purified using Streptavidin Magnesphere Paramagnetic beads. Their C-terminal fragments that bound to the beads were recovered after CASP3 cleavage and their sequences were determined. Using this approach, the cleavage sites of ACVR1, AKT2, BMPR1B, CaMKK1, HSPB8, MAPK12, MKNK2(D58), PDPK1, PRKCI, PRKX, RIOK1, RIOK3, and RPS6KA5 were determined. We then attempted to determine the cleavage sites of the remaining PKs by other methods.

The NCtagged PKs that had low biotin-labeling efficiencies and were cleaved near their C-termini were genetically modified by the addition of a glutathione-*S*-transferase (GST) fragment at their C-termini to facilitate recovery with

Table 1 Characteristics of the newly identified CASP3 PK substrates

Symbols	Kinome names	Groups	Clone origin	AA[a]	Cleavage sequence	Cleavage sites	Methods[b]	Conservation[c]	Smallest frag.[d]	*In vivo* cleavages[e]
ACVR1	ALK2	TKL	Hs	509	IASD↓M	269	NT	Yes	C240	Yes
AKT2	AKT2	AGC	Mm	481	DAMD↓Y	121	NT	Yes	N121	Yes
BMPR1B	ALK6	TKL	Hs	502	CSTD↓G	50	NT	Yes	N50	Yes
					DFVD↓G	120	NT	Yes		
CaMKK1	CaMKK1	Other	Hs	520	EEAD↓G	32	NT	Yes	N32	Yes
CSK	CSK	TK	Mm	450	DAPD↓G	409	MS	Yes	C41	Yes
CSNK1G1	CK1g1	CK1	Mm	459	VHVD↓S	343	MU	Yes	C116	Yes
eEF2K	eEF2K	Atypical	Hs	725	EGVD↓G	14	MU	Yes	N14	Yes
					DHLD↓N	430	MU	Yes		
HSPB8	H11	Atypical	Hs	196	MAD↓G	3	NT	Yes	N3	Yes
MAP2K6	MAP2K6	STE	Mm	334	DFVD↓F	289	MU	Yes	C45	Yes
MAPK12	p38g	CMGC	Hs	367	SAVD↓G	46	NT	Yes	N46	Yes
MARK1	MARK1	CAMK	Hs	795	SATD↓E	52	MU	Yes	N52	Yes
MKNK2	MNK2	CAMK	Hs	414	DQPD↓H	32	MU	No	N32	Yes
					DIPD↓A	58	NT	Yes		
PDPK1	PDK1	AGC	Hs	556	SHPD↓A	552	NT	Yes	C4	Yes
PIM2	PIM2	CAMK	Hs	334	TDFD↓G	198	MU	Yes	C113	Yes
PRKAA1	AMPKa1	CAMK	Hs	550	TSLD↓S	520	MS	Yes	C30	Yes
PRKCI	aPKCi	PKC	Hs	596	TQRD↓S	6	NT	Yes	N6	Yes
PRKX	PRKX	AGC	Hs	358	ETPD↓G	25	NT	No	N25	Yes
RIOK1	RIOK1	Atypical	Mm	568	EKDD↓I	37	NT	Yes	N37	Yes
RIOK3	RIOK3	Atypical	Hs	516	DTRD↓D	139	NT	Yes	N139	Yes
RPS6KA5	MSK1	AGC	Hs	549	DGGD↓G	20	NT	Yes	N20	Yes
					DELD↓V	344	NT	Yes		
					TEMD↓P	356	NT	Yes		
SNARK	NuaK2	CAMK	Hs	628	VSED↓S	546	MU	Yes	C82	Yes
TRIB3	TRB3	CAMK	Hs	358	VVPD↓G	338	NT	Yes	C20	Yes
ULK4	ULK4	Other	Hs	580	SQID↓S	473	MU	Yes	C107	Yes
DCAMKL2	DCAMKL2	CAMK	Hs	695	—	—	—	—	—	Yes
DYRK3	DYRK3	CMGC	Hs	568	—	—	—	—	—	ND
IRAK2	IRAK2	TKL	Mm	622	—	—	—	—	—	Yes
MASTL	MASTL	AGC	Hs	879	—	—	—	—	—	Yes
PCTK1	PCTAIRE1	CMGC	Hs	496	—	—	—	—	—	Yes
PTK9	A6	Atypical	Hs	384	—	—	—	—	—	Yes
TGFBR1	TGFBR1	TKL	Hs	426	—	—	—	—	—	Yes

Abbreviations: Hs, human clone; Mm, mouse clone; MS, mass spectroscopy; MU, mutation; ND, not determined; NT, N-terminal sequencing. [a]Length of amino acids. [b]Methods for determination of cleavage site. [c]Very similar site conserving the Asp (D) of the hydrolytic bond was found between human and mouse PKs (Yes), whereas no similar sites was done (No). [d]The smallest N (N) or C (C) fragment in the cleaved PKs. Number is the length of amino acids of the fragment. [e]Data from Figure 4.

glutathione Sepharose 4B beads after CASP3 cleavage. CASP3 cleavage of the PK-GSTs produced the same size N-terminal fragments as those of the corresponding CASP3-cleaved NCtagged PKs, indicating that the GST tags did not alter the positions of the cleavage sites. In addition, the sequences of the cleaved c-src tyrosine kinase (CSK) and AMP-activated kinase-a1 (AMPKa1) fragments were determined using MALDI/TOF-MS. Other PK constructs that were synthesized in small amounts were subjected to D→A mutagenesis to determine their cleavage sites. In total, 28 cleavage sites in 23 PKs were identified (Table 1). Identical or similar cleavage sites were found in the corresponding human and mouse PKs, except for those of PRKX (Supplementary Table S2). (Sequence analysis showed that mouse PRKX does not have the N-terminal region that is found in human PRKX.) Therefore, the CASP3-substrate kinome may be highly conserved in mammals.

We also analyzed the common sequence attributes among the 28 cleavage sites and found that CASP3 prefers the sequence, DXXD↓G (Figure 5a). The consensus PK cleavage site for CASP3 in the MEROPS database is DXXD↓X. In the NCtagged PK library, 208 of the 304 PKs contain a DXXDX sequence. However, only 33 PKs were cleaved by CASP3; therefore, to be cleaved by CASP3, the DXXDX sequence and a structural element –probably accessibility – are required.

Characterization of the newly identified PKs that were cleaved near their N- or C-termini. Interestingly, 16 out of the 23 PKs, for which cleavage sites were characterized, have cleavage sites within 60 residues of their N- or C-termini. We investigated whether these sites were also cleaved *in vivo* when apoptosis was induced by TNFα. For these experiments, CaMKK1, eEF2K, MNK2, AMPKa1, and TRIB3, which were cleaved *in vitro* at D32, D14, D32/D58, D520 (30 residues away from the C-terminus), and D338 (20 residues away from the C-terminus), respectively, were used (Figure 5b and Table 1). Their genes (wild type, WT) were each reconstructed with a V5 tag added at the end opposite the cleavage site. The genes for their D→A mutants (DA), and for the sequences of their longer CASP3-cleaved fragments (C3M), were also constructed and all were expressed in control and in apoptotic cells (Figure 5c). Cleavage of the WT PKs produced long fragments corresponding to C3M in apoptotic cells, whereas z-VAD-FMK blocked cleavage. These cleavages near the N- and

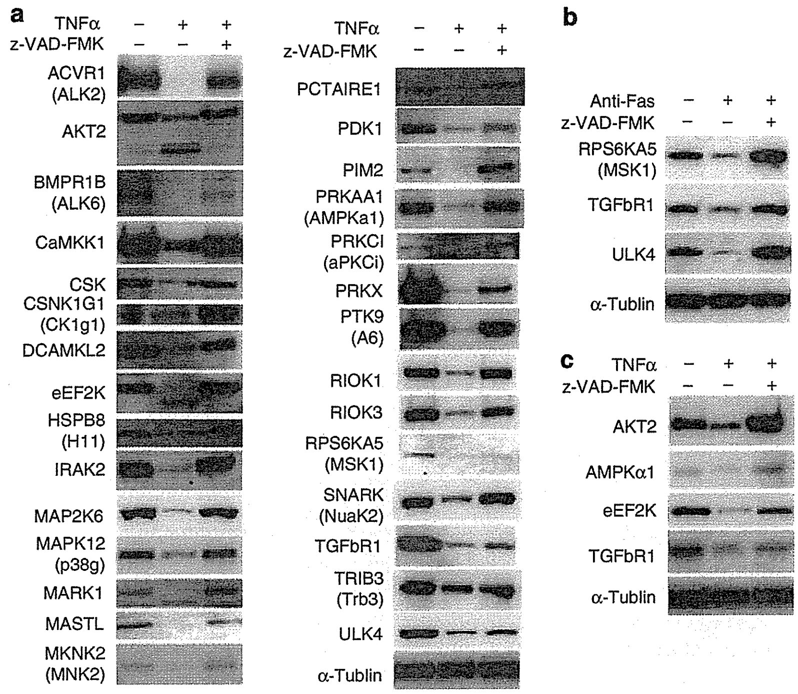

Figure 4 *In vivo* caspase cleavage of the newly identified PK substrates and of endogenous PK substrates. (**a**) *In vivo* cleavage of the $(His)_6$-PK-Flag constructs expressed in apoptotic HeLa cells. The cells were treated with DMSO (control) or with TNFα and cycloheximide (TNFα) in the presence and absence of z-VAD-FMK (a CASP3 inhibitor) for 6 h and then lysed. The cell extracts were immunoblotted and the PK constructs were detected with anti-Flag antibodies, except for HSPB8 and MAP2K6. Anti-His tag antibody was used for the two PKs. (**b**) The cells were transfected with a plasmid of $(His)_6$-PK-Flag constructs, and treated with DMSO (control), or with anti-Fas antibody (anti-Fas) in the presence and absence of z-VAD-FMK for 6 h and then lysed. Immunoblotting was carried out as (**a**). (**c**) HeLa cells were treated as in (**a**), but were not transfected with a *$(His)_6$-PK-Flag* gene. Each endogenous PK was detected using an antibody specific for it. α-Tubulin was used as an internal marker

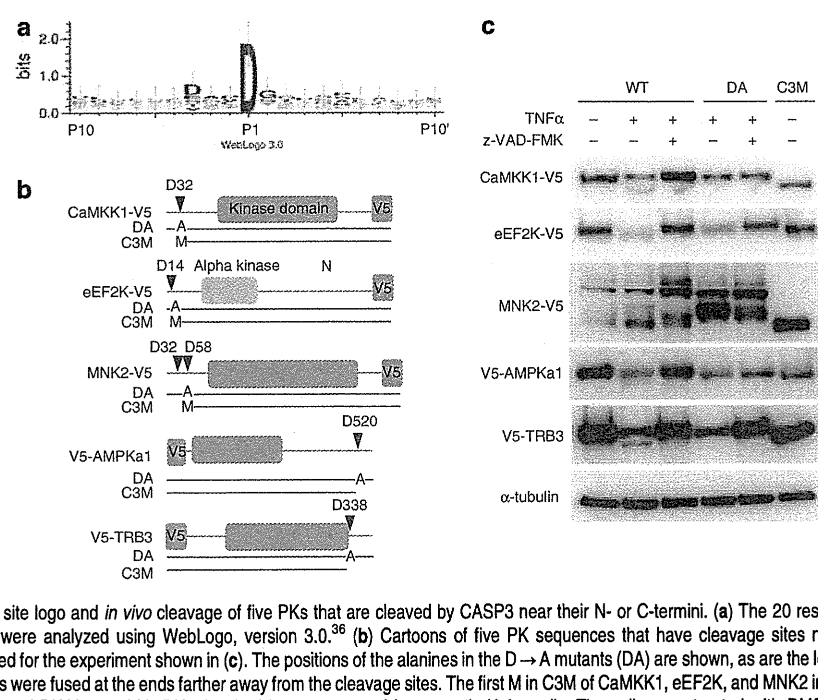

Figure 5 The cleavage site logo and *in vivo* cleavage of five PKs that are cleaved by CASP3 near their N- or C-termini. (**a**) The 20 residues surrounding the D of the hydrolytic bond in 28 PKs were analyzed using WebLogo, version 3.0.[36] (**b**) Cartoons of five PK sequences that have cleavage sites near their N- or C-termini. The corresponding PKs were used for the experiment shown in (**c**). The positions of the alanines in the D→A mutants (DA) are shown, as are the long fragments (C3M) produced by CASP3 cleavage. V5 tags were fused at the ends farther away from the cleavage sites. The first M in C3M of CaMKK1, eEF2K, and MNK2 indicates a methionine as a start amino acid. (**c**) Immunoblots of PK-V5s and V5-PKs that had been expressed in apoptotic HeLa cells. The cells were treated with DMSO (control) or with TNFα and cycloheximide in the presence or absence of z-VAD-FMK for 6 h and then lysed. The proteins were blotted and then detected with anti-V5 antibodies. WT indicates a wild-type protein

C-termini of the PKs suggest that CASP3 cleavage may regulate the activity level and/or cellular localization of the PKs, rather than simply inactivate the kinases.

Discussion

In 1995, PITSLRE,[29] PKCδ,[30] and DNA-PKcs[31] were reported as the first PK-type substrates of CASP3. During the next 15 years, 36 additional PKs that can be cleaved by CASP3 were found.[23,24,26] Notably, these authors showed that CASP3-cleaved PKs abrogate survival signals and accelerate apoptosis. In this study, we identified an additional 30 PKs that can be cleaved by CASP3. In addition, many of the cleavage sites were found in regulatory elements or in the regions near the N- and C-termini, rather than the kinase domain itself. Some of the newly identified CASP3-substrate PKs may be involved in apoptotic signal cascades. Sixteen PKs were shown to be cleaved *in vitro* near their N- or C-termini and at least five of them were also cleaved near their N- or C-termini in apoptotic cells (Figure 5). Using standard immunoblotting, proteins that are cleaved into a large and a small fragment may be overlooked because the mobilities of the large fragment and the intact protein will be nearly identical. Most of the PKs that had been previously reported to be cleaved by CASP3 were identified because the cleaved fragments had very different molecular weights than did the intact PK and were therefore easily detected by SDS-PAGE. Consequently, cleavages near the termini may have been overlooked. Taken together, our results suggest that CASP3 cleavage of some of the members of the CASP3-substrate kinome alters the function of the PKs and thereby signals apoptosis.

For the study reported herein, 304 out of 518 known PKs, synthesized as NCtagged PKs, were subjected to the *in vitro* cleavage assay (Supplementary Table S1). The relative number of PKs that were cleaved was ~14%. A total of 69 PKs that are CASP3 substrates are now known, which suggests that at least ~13% of the PKs in the human kinome are targets of CASP3. As ~200 PKs have yet be tested as CASP3 substrates, an additional 26 PKs (13% of the 200) may be CASP3 substrates. The human genome contains 518 annotated PKs, which have been divided into 10 groups on the basis of their sequence homologies.[3] Interestingly, the groups differ in terms of their susceptibilities to CASP3 cleavage (Table 2). Approximately 30% of the PKs in the AGC group are known CASP3 substrates, for example, AKT2, S6K, MSK, PKC, and PDK1. Many of the AGC-type PKs are commonly found in mammalian tissues,[32] and their cleavage sites are located in their regulatory domains (Figure 4 and Table 1). Therefore, these abundant PKs may be activated when CASP3 cleaves them and then act as intracellular apoptosis signals. Conversely, CASP3 cleaved only a relatively small number (6~8%) of the PKs in the CMGC group, which includes the kinases of the CDK and CDKL families, and the tyrosine kinase groups. Therefore, most members of these groups may only act indirectly as apoptosis signals after CASP3 activation.

Such ROCK1 and MST1, certain caspase cleavage products, work as apoptosis signaling.[23,24] In this study, we found at least six new CASP3 cleavage products, derived from AKT2, CaMKK1, eEF2K, MARK1, MNK2, and TRB3,

Table 2 Characteristics of the protein kinases used in this study

Groups	Total[a]	Tested clones	Cleaved clones (new[b])	Cleaved/test clones (%)
AGC	63	33	10 (6)	30
CAMK	74	52	8 (7)	15
CK1	12	8	1 (1)	13
CMGC	61	39	3 (3)	8
Other	83	46	3 (2)	7
STE	47	25	4 (1)	16
TK	90	51	3 (1)	6
TKL	43	27	6 (4)	22
RGC	5	2	0	0
Atypicals	40	21	5 (5)	24
Total	518	304	43 (30)	14

[a]Each number is corresponding to human kinome. [b]Newly PK numbers found in this study.

after 6 h from apoptosis induction (Figures 4 and 5). These cleavage products retain kinase domain, as in the case of ROCK1 and MST1. On the other hand, we could not detect any cleavage products from the other kinases *in vivo*. The reasons are not yet understood. However, recent proteomics approach has shown that the cleaved proteins displayed transient fragments in the apoptotic cells.[12] Further analysis at multiple time points during the apoptotic cascade would be required for detection of the cleavage products from the remaining PKs.

For TRIB3, full-length TRIB3 (D338A) mutant was decreased in apoptotic condition (compared TNFα lane with TNFα plus z-VAD-FMK lane in Figure 5c). However, the mutant could not produce the CASP3 cleavage product found as the shorter form in TNFα lane of WT, indicating that the mutant was not cleaved by CASP3. The mutant was also not cleaved by CASP3 *in vitro* (data not shown). As TRIB3 has been known to receive proteasomal degradation,[33] this unexpected reduction of the mutant TRIB3 in the apoptotic cells may be the effects of cycloheximide and/or caspase-inhibitor treatment on TRIB3 degradation.

Proteases often modify the activities of their targeted protein substrates. Identification of the specific substrate that is cleaved by a protease is necessary if the functions of both the protease and its substrate are to be understood. Proteomic studies have used mass spectrometry to exhaustively identify cellular proteins that have been cleaved by proteases.[11,12] However, it has been difficult to correlate specific proteases with their substrates because many proteases act at the same time *in vivo*.

Many full-length cDNAs derived from the genes of higher eukaryotes are available from many different sources. These cDNAs are potentially a great DNA template resource for *in vitro* syntheses of proteins. As a protein production system and for the functional analysis of proteins, the wheat cell-free system has many advantages: It can effectively use PCR-generated DNA templates.[14] It is easily adapted to an automated system.[15] It can be used to incorporate a single label into target proteins.[20] Its synthesized proteins do not require purification before being assayed, and it has no detectable proteasome activity.[21] In addition, the screening cost is very low (~US$1/assay), which for our study translated to 10 cents to produce each NCtagged protein and

20 cents for the beads, CASP3, and disposable hardware used in one assay.

In summary, we showed that an NCtagged PK library synthesized in a cell-free system could be used to characterize a CASP3-substrate kinome. Analysis of the CASP3-cleavage sites indicated that CASP3 cleavage of PKs depends on both primary and tertiary structure. Almost all of the PK substrates that we identified *in vitro* were also identified *in vivo*. Systems similar to that used herein could be used to screen other protease substrates.

Materials and Methods

General. The following procedures have been described:[14–16,20–22,34] wheat cell-free protein production; split-primer PCR synthesis of the DNA templates; parallel syntheses of mRNAs and their translated proteins; and measurements of the amounts of protein synthesized using densitometer scans of Coomassie brilliant blue-stained proteins or of radiolabeled proteins.

Construction of DNA templates for the expression of a PK protein library. The cloned genes encoding the PKs used in this study are listed in Supplementary Table S1. Their open-reading frames (without stop codons) were modified in two steps using PCR and the primers S1 (5′-CCACCCACCAC CACCAatg$(n)_{16}$-3′) and T1 (5′-TCCAGCACTAGCTCCAGA$(n)_{19}$-3′) (lowercase letters indicate nucleotides of the gene) for the first step, and the primers attB1-Flag-S1 (5′-GGGGACAAGTTTGTACAAAAAAGCAGGCTTCATGGACTACAAG GATGACGATGACAAGCTCCACCCACCACCACCAATG-3′) and T1-bls-STOP-attB2-anti (5′-GGGGACCACTTTGTACAAGAAAGCTGGGTTTATTCGTGCCACTC GATCTTCTGGGCCTCGAAGATGTCGTTCAGGCCGCTTCCAGCACTAGCTCCA GA-3′) for the second step. The PCR-modified genes were each inserted into a pDONR221 vector using the Gateway BP Clonase II enzyme mix (Invitrogen, Carlsbad, CA, USA) to give pDONR-Flag-PK-bls vectors. *Escherichia coli* cells were transformed with these vectors and then cultured in wells of a 96-well plate that contained GYT medium (10% (v/v) glycerol, 0.125% (w/v) yeast extract, and 0.25% (w/v) tryptone) for 48 h without shaking. DNA templates for mRNA and protein expression were constructed using split-primer PCR[14] in two steps. For the first step, the pDONR221-Flag-PK-bls plasmids that had not been isolated from the *E. coli* cells, and the primers pDONR221-1st_4080 (5′-ATCTTTTCTACGGGGT CTGA-3′) and deSP6E02-Flag-S1 (5′-GGTGACACTATAGAACTCACCTATCTC TCTACACAAAACATTTCCCTACATACAACTTTCAACTTCCTATTATGGACTACAA GGATGACGATGACAAGCTCCACCCACCACCACCAATG-3′) were used, and for the second step, the amplified sequences of the first step and the primers SPu (5′-GGGTAGCATTTAGGTGACACT-3′) and pDONR221-2nd_4035 (5′-ACGTTAA GGGATTTTGGTCA-3′) were used to give SP6-E02-Flag-PK-bls DNA templates. (The E02 sequence is a translational enhancer,[35] and the SP6 sequence is an SP6 RNA polymerase promoter.)

Cell-free protein synthesis. Cell-free protein synthesis used the reagents of an ENDEXT Wheat Germ Expression S Kit according to the manufacturer's instructions (CellFree Sciences Co., Ltd.), the bilayer translation method,[15,16,34] and a robotic synthesizer (GenDecorder 1000; CellFree Sciences). Each DNA template was transcribed by SP6 RNA polymerase, then precipitated with ethanol, and collected by centrifugation (15 000 r.p.m. for 5 min., R10H rotor; Hitachi). Each mRNA ($\sim$30–35 μg) was washed with 75% ethanol, added into a translation mixture, and translated in the bilayer mode[31] with the following modifications. The translation mixture (25 μl) (bottom layer) contained 60 A_{260}/ml of ENDEXT wheat germ extract, 1 $\times$ SUB-AMIX (24 mM Hepes-KOH, pH 7.8, 1.2 mM ATP, 0.25 mM GTP, 16 mM creatine phosphate, 2.5 mM DTT, 0.4 mM spermidine, 0.3 mM each of the 20 amino acids, 2.8 mM magnesium acetate, 100 mM potassium acetate), 2 μg creatine kinase (Roche Applied Science, Indianapolis, IN, USA), 500 nM D-biotin (Nacalai Tesque, Kyoto, Japan), and 1 μl of the wheat cell-free translational mixture that expressed BirA biotin ligase ($\sim$50 ng/μl, BirA: GenBank Accession No. NP_0312927). A 1 $\times$ SUB-AMIX solution (125 μl) was placed over the translation mixture. The bilayer was incubated at 26°C for 17 h to allow for protein synthesis. All steps including construction of the DNA templates were performed in the wells of a 96-well plate.

Cleavage assay. The cell-free-synthesized PKs that had luminescent signals $>$500 units (in the absence of CASP3) were studied. For each PK, 10 μl of the CASP3 cleavage buffer (20 mM Tris-HCl, pH 7.5, 0.2 mM DTT, 5 mM $MgCl_2$, 3 mM ATP, 1 mg/ml BSA, 1 mU CASP3 (Sigma-Aldrich, St. Louis, MO, USA)) was mixed with 1 μl of the translation mixture that contained a Flag-PK-bls$\sim$biotin construct, and the mixture was incubated at 30°C for 2 h in a well of a 384-well Optiplate (Perkin Elmer, Foster City, CA, USA). Using the reagents of an AlphaScreen IgG (protein A) detection kit (Perkin Elmer) according to the manufacturer's instructions, 15 μl of 20 mM Tris-HCl, pH 7.5, 0.2 mM DTT, 5 mM $MgCl_2$, 5 μg/ml anti-FLAG M2 antibody (Sigma-Aldrich), 1 mg/ml BSA, 0.1 μl of streptavidin-coated donor beads and 0.1 μl of anti-IgG acceptor beads were added to the well. The solution was incubated at 23°C for 1 h. Luminescence was analyzed using the AlphaScreen detection program (Perkin Elmer). All repetitive mechanical procedures were performed by a Biomek FX robotic workstation (Beckman Coulter, Fullerton, CA, USA). The value of a luminescent signal is reported as the mean of three independent measurements.

TD immunoblotting. A mixture of each Flag-PK-bls$\sim$biotin construct (3 μl of a translation mixture) and 7 μl of the CASP3 cleavage solution was incubated at 30°C for 1 h in a well of a 384-well Optiplate (Perkin Elmer). Then, the proteins were separated in SDS-PAGE gels and transferred to PVDF membranes (Millipore Bedford, MA, USA). The blotted proteins were prepared for detection using the reagents of an ECL-Plus Western Blotting Detection System kit (GE Healthcare, Piscataway, NJ, USA), anti-Flag M2 antibodies (Sigma-Aldrich) for N-TD, and Alexa488-streptavidin (Invitrogen) for C-TD. The labeled proteins were visualized using a Typhoon Imager (GE Healthcare) with a 532-nm laser and a 526-nm emission filter or an ImageQuant LAS-4000 mini CCD camera system (Fujifilm).

Sequencing and other purification procedures. When possible, long biotinylated C-terminal fragments produced by CASP3 cleavage were recovered attached to streptavidin beads, and then sequenced directly. When a PK construct had a low biotin-labeling efficiency and was cleaved near its C-terminus, a new construct was made by fusing the GST nucleotide sequence encoded in the pEU-E01-Gateway-GST vector to the C-terminal codon of the corresponding PK open-reading frame using the Gateway system and the pEU-E01-Gateway-GST vector. For purification, synthesized PKs (1.2 ml) were purified using Streptavidin Magnesphere Paramagnetic beads (Promega Corp., Madison, WI, USA) for the Flag-PK-bls$\sim$biotin constructs or glutathione Sepharose 4B (GE Healthcare) for the PK-GST constructs. After washing the beads with PBS, the bound PKs were incubated with CASP3 (15 μl of total volume) as described above. The samples were boiled and the proteins separated by SDS-PAGE. After blotting and visualization (ProBlott, Applied Biosystems, Foster City, CA, USA), the membrane areas that contained the cleaved fragments were cut out and the fragments were sequenced (Applied Biosystems ABI 473A). CSK kinase (Carna Biosciences Inc., Kobe, Japan) and AMPKa1 (Cell Signaling Technology, Beverly, MA, USA) were cleaved with CASP3 (10 μl of total volume), and the cleavage products subjected to MALDI/TOF-MS (Shimazu Techno-Research Inc., Kyoto, Japan) for sequencing. D$\rightarrow$A mutagenesis was carried out using the reagents of a PrimeSTAR Mutagenesis Basal kit (TakaraBio, Otsu, Japan) according to the manufacturer's instructions. The mutated genes were sequenced using an ABI PRISM 310 DNA sequencer (Applied Biosystems).

Construction of PK expression plasmids for the cell-based assay. Expression plasmids were produced using the Gateway method. To obtain the attB1-PK-Flag-(stop codon)-attB2 for Gateway BP Clonase II recombination, the open-reading frame products of the 30 newly identified PK substrates of CASP3 that had been produced by PCR using the S1 and T1 primers as described above were PCR amplified using the primers, attB1-S1 (5′-GGGGACAAGTTTGTA CAAAAAAGCAGGCTTCCACCCACCACCACCA-3′) and T1-Flag-stop-attB2 (5′-GGGGACCACTTTGTACAAGAAAGCTGGGTTTACTTGTCATCGTCATCCTTG TAGTCGCTTCCAGCACTAGCTCCAGA-3′). These PCR products were each inserted into a pDEST26 vector (Invitrogen) using the Gateway system for construction of the His-PK-Flag nucleotide sequences. All sequences were confirmed by DNA sequencing as described above.

Cell-based assay. HeLa cells were cultured in Dulbecco's modified Eagle's medium, 10% fetal bovine serum, penicillin (100 mg/ml), and streptomycin (50 μg/ml). Transient transfections were carried out using Lipofectamine 2000 Transfection Reagent (Invitrogen) according to the manufacturer's instructions. At 24 h after transfection, cells were harvested after apoptosis was induced. Control cells were treated with DMSO and, for apoptosis induction or inhibition, with 20 ng/ml TNFα

(Calbiochem, La Jolla, CA, USA) and 100 μM cycloheximide (Chemicon, Temecula, CA, USA) or 125 ng/ml anti-Fas antibody (Medical & Biological Laboratories Co., Ltd., Nagoya, Japan) in the presence (inhibition) or absence (induction) of 100 μM Z-VAD-FMK (Peptide Institute Inc., Osaka, Japan) for 6 h. Cells were washed with PBS and then lysed directly by adding one volume of 2 × SDS-PAGE sample buffer (125 mM Tris-HC1, pH 6.8, 20% glycerol, 4% SDS, 10% 2-mercaptoethanol, 0.001% bromphenol blue) before subjecting the cell extracts to SDS-PAGE and immunoblotting, which used anti-His antibodies (GE Healthcare) or anti-Flag M2 antibodies (Sigma-Aldrich). The following antibodies were employed to detect endogenous proteins: anti-α-tubulin (Sigma-Aldrich); anti-AKT2, anti-eEF2K, anti-AMPKa1, and anti-TGFbR1 (Cell Signaling Technology). Chemiluminescent signals, generated by ECL-Plus reagents (GE Healthcare), or Immobilon Western HRP substrate Luminol Reagent (Millipore), were detected using an LAS-4000mini biomolecular imager (GE Healthcare).

Conflict of interest

Dr. Endo is a founder of CellFree Sciences Co., Ltd. and a member of its scientific advisory board. Other authors declare no conflict of interest.

Acknowledgements. We thank Professor Akihide Ryo (Yokohama City University, Japan) for his useful comments and suggestions concerning the cell analysis, Mr. Tatsuya Akagi for technical assistance, and Dr. Morishita (CellFree Sciences) for assistance with the robotic operations. This work was partially supported by the Special Coordination Funds for Promoting Science and Technology by the Ministry of Education, Culture, Sports, Science, and Technology, Japan (Nos. 19657041 and 22310127 to TS).

1. Puente XS, Sanchez LM, Overall CM, Lopez-Otin C. Human and mouse proteases: a comparative genomic approach. *Nat Rev Genet* 2003; **4**: 544–558.
2. Hunter T. Signaling – 2000 and beyond. *Cell* 2000; **100**: 113–127.
3. Manning G, Whyte DB, Martinez R, Hunter T, Sudarsanam S. The protein kinase complement of the human genome. *Science* 2002; **298**: 1912–1934.
4. Matrisian LM, Hogan BL. Growth factor-regulated proteases and extracellular matrix remodeling during mammalian development. *Curr Top Dev Biol* 1990; **24**: 219–259.
5. Turgeon VL, Houenou LJ. The role of thrombin-like (serine) proteases in the development, plasticity and pathology of the nervous system. *Brain Res Brain Res Rev* 1997; **25**: 85–95.
6. van Kempen LC, de Visser KE, Coussens LM. Inflammation, proteases and cancer. *Eur J Cancer* 2006; **42**: 728–734.
7. Friedl P, Wolf K. Tube travel: the role of proteases in individual and collective cancer cell invasion. *Cancer Res* 2008; **68**: 7247–7249.
8. Abdel-Rahman HM, Kimura T, Hidaka K, Kiso A, Nezami A, Freire E *et al.* Design of inhibitors against HIV, HTLV-I, and *Plasmodium falciparum* aspartic proteases. *Biol Chem* 2004; **385**: 1035–1039.
9. Alnemri ES. Mammalian cell death proteases: a family of highly conserved aspartate specific cysteine proteases. *J Cell Biochem* 1997; **64**: 33–42.
10. Hengartner MO. The biochemistry of apoptosis. *Nature* 2000; **407**: 770–776.
11. Mahrus S, Trinidad JC, Barkan DT, Sali A, Burlingame AL, Wells JA. Global sequencing of proteolytic cleavage sites in apoptosis by specific labeling of protein N termini. *Cell* 2008; **134**: 866–876.
12. Dix MM, Simon GM, Cravatt BF. Global mapping of the topography and magnitude of proteolytic events in apoptosis. *Cell* 2008; **134**: 679–691.
13. Righetti PG, Boschetti E. Sherlock Holmes and the proteome – a detective story. *FEBS J* 2007; **274**: 897–905.
14. Sawasaki T, Ogasawara T, Morishita R, Endo Y. A cell-free protein synthesis system for high-throughput proteomics. *Proc Natl Acad Sci USA* 2002; **99**: 14652–14657.
15. Sawasaki T, Morishita R, Gouda MD, Endo Y. Methods for high-throughput materialization of genetic information based on wheat germ cell-free expression system. *Methods Mol Biol* 2007; **375**: 95–106.
16. Takai K, Sawasaki T, Endo Y. Practical cell-free protein synthesis system using purified wheat embryos. *Nat Protoc* 2010; **5**: 227–238.
17. Endo Y, Sawasaki T. Cell-free expression systems for eukaryotic protein production. *Curr Opin Biotechnol* 2006; **17**: 373–380.
18. Sawasaki T, Hasegawa Y, Morishita R, Seki M, Shinozaki K, Endo Y. Genome-scale, biochemical annotation method based on the wheat germ cell-free protein synthesis system. *Phytochemistry* 2004; **65**: 1549–1555.
19. Goshima N, Kawamura Y, Fukumoto A, Miura A, Honma R, Satoh R *et al.* Human protein factory for converting the transcriptome into an *in vitro*-expressed proteome. *Nat Methods* 2008; **5**: 1011–1017.
20. Sawasaki T, Kamura N, Matsunaga S, Saeki M, Tsuchimochi M, Morishita R *et al.* Arabidopsis HY5 protein functions as a DNA-binding tag for purification and functional immobilization of proteins on agarose/DNA microplate. *FEBS Lett* 2008; **582**: 221–228.
21. Takahashi H, Nozawa A, Seki M, Shinozaki K, Endo Y, Sawasaki T. A simple and high-sensitivity method for analysis of ubiquitination and polyubiquitination based on wheat cell-free protein synthesis. *BMC Plant Biol* 2009; **9**: 39.
22. Matsuoka K, Komori H, Nose M, Endo Y, Sawasaki T. Simple screening method for autoantigen proteins using the N-terminal biotinylated protein library produced by wheat cell-free synthesis. *J Proteome Res* 2010; **9**: 4264–4273.
23. Fischer U, Janicke RU, Schulze-Osthoff K. Many cuts to ruin: a comprehensive update of caspase substrates. *Cell Death Differ* 2003; **10**: 76–100.
24. Kurokawa M, Kornbluth S. Caspases and kinases in a death grip. *Cell* 2009; **138**: 838–854.
25. Lee KK, Murakawa M, Nishida E, Tsubuki S, Kawashima S, Sakamaki K *et al.* Proteolytic activation of MST/Krs, STE20-related protein kinase, by caspase during apoptosis. *Oncogene* 1998; **16**: 3029–3037.
26. Tomiyoshi G, Horita Y, Nishita M, Ohashi K, Mizuno K. Caspase-mediated cleavage and activation of LIM-kinase 1 and its role in apoptotic membrane blebbing. *Genes Cells* 2004; **9**: 591–600.
27. Tatsuta T, Shiraishi A, Mountz JD. The prodomain of caspase-1 enhances Fas-mediated apoptosis through facilitation of caspase-8 activation. *J Biol Chem* 2000; **275**: 14248–14254.
28. Packard BZ, Komoriya A, Brotz TM, Henkart PA. Caspase 8 activity in membrane blebs after anti-Fas ligation. *J Immunol* 2001; **167**: 5061–5066.
29. Lahti JM, Xiang J, Heath LS, Campana D, Kidd VJ. PITSLRE protein kinase activity is associated with apoptosis. *Mol Cell Biol* 1995; **15**: 1–11.
30. Emoto Y, Manome Y, Meinhardt G, Kisaki H, Kharbanda S, Robertson M *et al.* Proteolytic activation of protein kinase C delta by an ICE-like protease in apoptotic cells. *EMBO J* 1995; **14**: 6148–6156.
31. Casciola-Rosen LA, Anhalt GJ, Rosen A. DNA-dependent protein kinase is one of a subset of autoantigens specifically cleaved early during apoptosis. *J Exp Med* 1995; **182**: 1625–1634.
32. Pearce LR, Komander D, Alessi DR. The nuts and bolts of AGC protein kinases. *Nat Rev Mol Cell Biol* 2010; **11**: 9–22.
33. Ohoka N, Sakai S, Onozaki K, Nakanishi M, Hayashi H. Anaphase-promoting complex/cyclosome-cdh1 mediates the ubiquitination and degradation of TRB3. *Biochem Biophys Res Commun* 2010; **392**: 289–294.
34. Sawasaki T, Hasegawa Y, Tsuchimochi M, Kamura N, Ogasawara T, Kuroita T *et al.* A bilayer cell-free protein synthesis system for high-throughput screening of gene products. *FEBS Lett* 2002; **514**: 102–105.
35. Kamura N, Sawasaki T, Kasahara Y, Takai K, Endo Y. Selection of 5′-untranslated sequences that enhance initiation of translation in a cell-free protein synthesis system from wheat embryos. *Bioorg Med Chem Lett* 2005; **15**: 5402–5406.
36. Crooks GE, Hon G, Chandonia JM, Brenner SE. WebLogo: a sequence logo generator. *Genome Res* 2004; **14**: 1188–1190.

Supplementary Information accompanies the paper on Cell Death and Disease website (http://www.nature.com/cddis)

technical notes Journal of proteome research

Simple Screening Method for Autoantigen Proteins Using the N-Terminal Biotinylated Protein Library Produced by Wheat Cell-Free Synthesis

Kazuhiro Matsuoka,[†] Hiroaki Komori,[‡,§] Masato Nose,[‡,||] Yaeta Endo,[*,†,||,⊥,#] and Tatsuya Sawasaki[*,†,||,⊥,#]

Cell-Free Science and Technology Research Center, Ehime University, 3 Bunkyo-cho, Matsuyama, Ehime 790-8577, Japan, Department of Pathogenomics, Ehime University Graduate School of Medicine, Toon, Ehime 791-0295, Japan, Proteo-Medicine Research Center, Ehime University, Toon, Ehime 791-0295, Japan, The Venture Business Laboratory, Ehime University, 3 Bunkyo-cho, Matsuyama, Ehime 790-8577, Japan, and RIKEN Systems and Structural Biology Center, 1-7-22 Suehiro-cho, Tsurumi-ku, Yokohama, Kanagawa 230-0045, Japan

Received November 18, 2009

Abstract: Autoimmune diseases are a heterogeneous group of diseases characterized by immune reactions against either a major or a limited number of the bodies own autoantigens, causing inflammation and damage to tissues and organs. Thus, identification of autoantigens is an important first step to understanding autoimmune diseases. Here we demonstrate a simple screening method for identification of autoantigens reacting with patient serum antibodies by combination of an N-terminal biotinylated protein library (BPL), produced using a wheat cell-free protein production system, and a commercially available luminescence system. Optimization studies using well-characterized autoantigens showed specific interactions between N-terminal biotinylated proteins and antibody that were sensitively detected under homogeneous reaction conditions. In this optimized assay, 1 μL of the translation mixture expressing the biotinylated proteins produced significant luminescence signal by addition of diluted serum between 1:500 and 1:10 000 in 25 μL of reaction volume. For the BPL construction, 214 mouse genes, consisting of 103 well-known autoantigens and 111 genes in the mouse autoimmune susceptibility loci, and the sera of MRL/lpr mouse were used as an autoimmune model. By this screening method, 25 well-known autoantigens and 71 proteins in the loci were identified as autoantigen proteins specifically reacting with sera antibodies. Cross-referencing with the Gene Ontology Database, 26 and 38 of autoantigen proteins were predicted to have nuclear localization and identified as membrane and/or extracellular proteins. The immune reaction of six randomly selected proteins was confirmed by immunoprecipitation and/or immunoblot analyses. Interestingly, three autoantigen proteins were recognized by immunoprecipitation but not by immunoblot analysis. These results suggest that the BPL-based method could provide a simple system for screening of autoantigen proteins and would help with identification of autoantigen proteins reacting with antibodies that recognize folded proteins, rather than denatured or unfolded forms.

Keywords: autoantigen • autoimmunity • biomarker • cell-free protein production • Gene Ontology • high-throughput screening • MRL/lpr mouse • proteomics

Introduction

Autoimmune diseases are generally characterized by the body's immune responses being directed against its own tissues, causing prolonged inflammation and subsequent tissue destruction.[1] A hallmark of autoimmune diseases is the production of autoantibodies such as antinuclear, anti-Sm and anti-dsDNA in systemic lupus erythematosus (SLE),[2] and the presence of RF, hnRNP A2 and calpastatin in rheumatoid arthritis (RA).[3] However, there are still a lot of autoimmune diseases for which antibodies have not been identified.[2] To understand the molecular mechanisms in autoimmune diseases, it is important to identify the relevant autoantigens, and moreover, they could be pathogenic in these diseases. It is widely hypothesized that proteins are the major antigenic targets associated with autoimmune diseases.[2] Therefore, development of methods that allow large-scale screening of autoantigen proteins is indispensable for elucidation and diagnosis of the autoimmune diseases.

To date, autoantigen proteins have been detected as antigenic molecules that are recognized by humoral antibodies, including those in serum.[2] The large-scale screening of au-

* To whom correspondence should be addressed. Yaeta Endo, Cell-Free Science and Technology Research Center, Ehime University, Bunkyo-cho, 3-ban, Matsuyama 790-8577, Japan. Tel. +81-89-927-9936. Fax +81-89-927-9941. E-mail yendo@eng.ehime-u.ac.jp. Tatsuya Sawasaki, Cell-Free Science and Technology Research Center, Ehime University, Bunkyo-cho, 3-ban, Matsuyama 790-8577, Japan. Tel. +81-89-927-8530. Fax +81-89-927-9941. E-mail sawasaki@eng.ehime-u.ac.jp.

† Cell-Free Science and Technology Research Center, Ehime University.

‡ Ehime University Graduate School of Medicine.

§ Deceased March 7, 2009.

|| Proteo-Medicine Research Center, Ehime University.

⊥ The Venture Business Laboratory, Ehime University.

RIKEN Systems and Structural Biology Center.

Published on Web 06/24/2010

10.1021/pr9010553

toantigen proteins reacting with patient serum antibodies has been carried out by mainly three technologies: serological proteome analysis (SERPA), serological expression cloning (SEREX) and protein microarray.[4] The utility of SERPA and SEREX for this screening is limited because particular cells and tissues are generally used as antigen resources in these systems and they are dependent on artificial membranes for immunoblotting which do not maintain native protein structure.[5] Recent advances in protein microarray technology have allowed large-scale screening of autoantigens reacting with the sera of patients suffering from autoimmune disorders and cancer.[5−7] However, protein microarray is not yet a commonly used biochemical tool for screening.[8] One issue with protein microarrays is that purified recombinant proteins are required, which demonstrate batch-to-batch variation and limited stability and shelf life.[5] Additionally, it is difficult to maintain the functional form of a protein after their immobilization on a microplate. Many proteins needed to be appropriately oriented for proper functioning.[9] In fact, a number of spotted autoantigens were not always detectable with planar arrays, presumably due to loss of three-dimensional structures, steric interference or electrostatic repulsion.[6]

In this work, we developed a novel autoantigen protein screening method that overcame the following issues highlighted above: (1) utilization of a high-throughput and genome-wide protein expression system, (2) specific protein labeling for assay using unpurified protein samples and (3) high-throughput detection system of properly folded antigen. Toward the first, we recently developed an automated protein production robot utilizing a high-throughput wheat embryo derived cell-free protein production system.[10,11] The combination of an automatic cell-free protein production system and the full-length cDNA allowed for facile construction of a robust protein library.[12] To enhance the utility of the library, per the second issue above, specific labeling of each protein is required for efficient detection. We selected biotin as the labeling compound because it is readily available and demonstrates high specificity for streptavidin binding. The biotinylated protein library (BPL) was constructed using target proteins fused to a biotin ligation site (bls), and expression was performed in the presence of biotin and biotin ligase (BirA).[13] BirA from *Escherichia coli* specifically conjugates a single biotin on the bls. This method was compatible with our high-throughput automated platform. To address the third issue, we selected the luminescent high-throughput protein−protein interaction detection system AlphaScreen.[14,15] This method can directly recognize biotinylated protein in the translation mixture without purification and the use of any potential protein denaturants allowing for antibody detection of natively folded antigens.[15] In this work, we demonstrate a simple BPL-based method for screening of autoantigen proteins reacting with the sera of an autoimmune disease model mouse, MRL/Mp-*lpr/lpr* (MRL/lpr), and the detection of the autoantigen proteins by immunoprecipitation, rather than immunoblotting methods often accompanied by protein denaturation.

Materials and Methods

General. The following procedures have been either described in detail or cited previously:[10,16] generation of DNA template by polymerase chain reaction (PCR) using "split-primer"; synthesis of mRNA and protein in parallel; estimation of the amounts of synthesized proteins by densitometric scanning of the Coomassie brilliant blue (CBB)-stained bands or by autoradiography. The wheat germ extract was purchased from Cell-Free Science Co. (Yokohama, Japan). Anti-p53 monoclonal antibody (D01) was purchased from Santa Cruz Biotechnology (Santa Cruz, CA). Mouse serum for mouse immunoglobulin in Figure 1 was purchased from Calbiochem (Darmstadt, Germany). Other reagents used in this study were described previously.[10,15]

Serum Samples. MRL/lpr mice were originally purchased from the Jackson Laboratory (Bar Harbor, ME). All of the mice used in this paper were maintained in clean rooms at the Animal Research Institute, School of Medicine, Ehime University. Sera of female mice were collected from 15 mice and pooled and stocked in −20 °C until use. All experiments were done according to the Guidelines for the Care and Use of Laboratory Animals at Ehime University.

DNA Template Construction for the BPL. Functional annotation of mouse (FANTOM) as a mouse full-length cDNA resource is purchased from a company (Danaform, Tokyo, Japan). The DNA templates for transcription were constructed by "split-primer" PCR technique described previous reports.[10,17] The first PCR was amplified with 10 nM of each of the following primers: a gene specific primer, 5′- CCACCCACCACCACCAAT-Gnnnnnnnnnnnnnnnnnn (n denotes the coding region of the target gene), and AODA2303 (5′-GTCAGACCCCGTAGAAAAGA) or AODS (5′-TTTCTACGGGGTCTGACGCT). The second PCR products for protein synthesis were constructed with 100 nM SPu 5′-GCGTAGCATTTAGGTGACACT, 1 nM deSP6E02bls-S1 (5′-GGTGACACTATAGAACTCACCTATCTCTCTACACAAAACA-TTTCCCTACATACAACTTTCAACTTCCTATTATGGGCCTGAAC-GACATCTTCGAGGCCCAGAAGATCGAGTGGCACGAACTCCA-CCCACCACCACCAATG) and 100 nM AODA2303 or AODS. By this "split-primer" PCR, the bls was fused onto the N-terminals of all the genes for protein biotinylation.[13]

Construction of the BPL by the Cell-Free Protein Synthesis System. Cell-free construction of the BPL is based on the previously described bilayer diffusion system in which 1 μL (50 ng) crude cell-free expressed BirA was added to the translation layer and 500 nM D-biotin (Nacalai Tesque, Kyoto, Japan) was added to both the translation and substrate layers.[13,18] *In vitro* transcription and cell-free protein synthesis for the BPL were carried out using the GenDecoder1000 robotic synthesizer (CellFree Sciences Co.) as previously described.[17,19]

Detection of Biotinylated Protein−Antibody Reaction by Luminescence Method. The AlphaScreen assay was performed according to the manufacture's protocol (PerkinElmer Life and Analytical Sciences, Boston, MA). Reactions were carried out in 25 μL of reaction volume in 384-well Optiwell microtiter plates (PerkinElmer Life and Analytical Sciences). For the antigen−autoantibody reaction, the translation mixture expressing the biotinylated protein was mixed with MRL/lpr mouse serum diluted 1:600 in 15 μL of reaction buffer [100 mM Tris-HCl (pH 8.0), 0.01% (v/v) Tween-20 and 0.1% (w/v) bovine serum albumin] and incubated at 26 °C for 30 min. Subsequently, 10 μL of streptavidin-coated donor beads and protein A-conjugated acceptor beads (PerkinElmer Life and Analytical Sciences) were added to a final concentration of 20 μg/mL per well and incubated at 26 °C for 1 h in a dark box. Fluorescence emission was measured with the EnVision plate reader (PerkinElmer Life and Analytical Sciences), and the resultant data were analyzed using the AlphaScreen detection program. All repetitive mechanical procedures were performed by a Biomek FX robotic workstation (Beckman Coulter, Fullerton, CA).

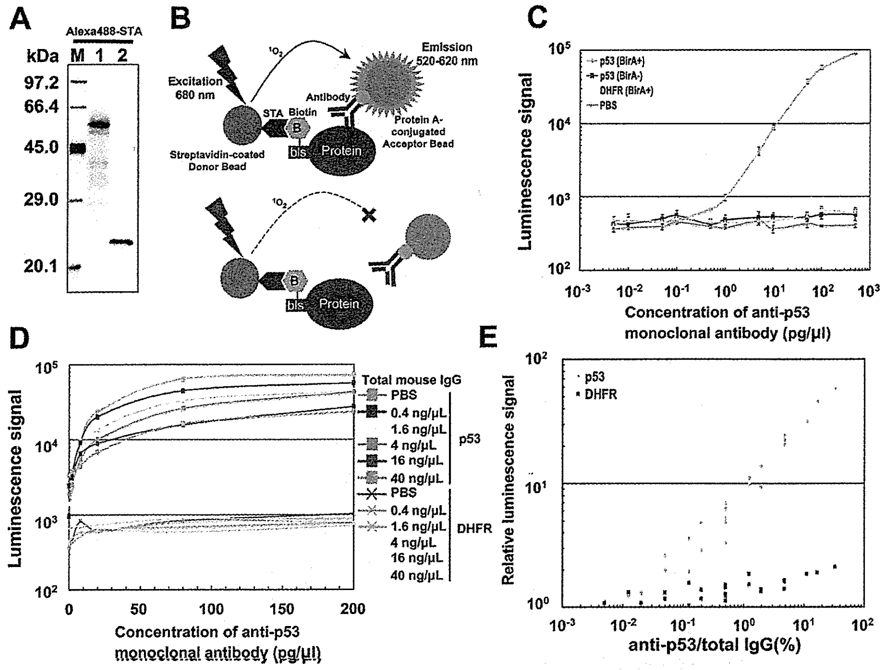

Figure 1. Sensitivity and specificity for detection of biotinylated p53 protein–antibody complex. (A) Biotinylated p53 (lane 1) and dihydrofolate reductase (DHFR) (lane 2) was detected by immunoblotting analysis using Alexa488-STA. M indicates protein molecular weight marker. (B) Schematic diagram of detection of biotinylated protein–antibody interaction by luminescence analysis. When a biotinylated protein and antibody interact (upper panel), Protein A-conjugated acceptor beads bound to antibody and streptavidin (STA)-coated donor beads bound to biotinylated protein are in close proximity. Upon excitation at 680 nm, a singlet oxygen is generated by the donor beads, transferred to the acceptor beads within 200 nm, and the resultant reaction emits light at 520–620 nm. This emission is measured using an EnVision. (C) Detection sensitivity of the antibody concentration measured by luminescence analysis. Translation mixture (1 μL) expressing biotinylated or nonbiotinylated p53 protein and biotinylated DHFR were incubated with various concentration of monoclonal antibody from 5×10^{-3} to 5×10^{2} pg/μL. (D) Biotinylated protein–antibody complex by interaction between biotinylated p53 protein and the monoclonal antibody in the presence of mouse serum was detected by luminescence analysis. (E) Minimum IgG amount in the presence of mouse serum to detect biotinylated p53 proteins. The relative luminescence signals between the specific luminescence and background signals indicated in the *y*-axis.

Immunoblotting. Biotinylated proteins were partially purified using streptavidin-coated beads (Streptavidin Sepharose High Performance, GE Healthcare, Buckinghamshire, U.K.). Translation mixtures (150 μL) including biotinylated proteins were mixed with 10 μL of streptavidin-coated beads for 30 min. The resin was washed three times with PBS buffer and then boiled in 15 μL of SDS sample buffer (50 mM Tris-HCl pH 6.8, 2% SDS, 10% glycerol and 0.2% bromophenol blue). After separation by 12.5% SDS-PAGE, the proteins were transferred to PVDF membrane (Millipore, Bedford, MA) by semidry blotting. The membrane was soaked in PBS containing 5% (w/v) skim milk for 1 h and then incubated with serum diluted 1:200 in PBS containing 0.1% (v/v) Tween 20 (PBST) for 1 h. After washing three times in PBST, it was incubated in PBS including goat-antimouse IgG-HRP antibody (GE Healthcare) diluted 1:10 000 for 30 min. After washing three times in PBST, the blots were detected by the ECL plus detection system (GE Healthcare) by using Typhoon 9400 imaging system (GE Healthcare) according to the manufacturer's protocol.

Immunoprecipitation. Fifty microliters of translation mixture expressing biotinylated proteins were incubated in 50 μL of IP buffer [PBS containing 0.1% (w/v) BSA, 0.15% (v/v) Tween 20] with 1 μL of undiluted serum overnight at 4 °C. Immobilized Protein A sepharose (20 μL of 50% slurry, Protein A Sepharose 4 Fast Flow, GE Healthcare) in IP buffer was added to each sample and incubated for 60 min at 4 °C. After centrifugation for 1 min at 900× *g*, samples were washed three times with IP buffer and then boiled for 5 min in SDS sample buffer. After separation by 12.5% SDS-PAGE, the samples were transferred to a Hybond-LFP PVDF membrane (GE Healthcare). After blocking with 5% (w/v) skim milk in PBS overnight at 4 °C, the membranes were soaked in PBS buffer containing 10 μg/mL streptavidin Alexa Fluor 488 conjugate (Alexa488-STA) (Invitrogen, Carlsbad, CA) and were washed three times with PBST. The biotinylated proteins on membrane were detected by Typhoon 9400 imaging system (GE Healthcare) according to the manufacturer's protocol.

Results

Sensitivity and Specificity for Detection of Antigen–Antibody Interaction Using Biotinylated p53 Protein. We adapted that AlphaScreen technology toward detecting interactions between antigen protein and antibody. To validate this technique, we used p53 protein, a well-characterized antigen protein.[20] Biotinylated or nonbiotinylated recombinant p53 and biotinylated recombinant dihydrofolate reductase (DHFR), serving as negative control, were synthesized by the wheat cell-free system (Figure 1A). For the analysis of antigen protein–antibody interaction, the translation mixture was used without any purification. In the AlphaScreen system, interaction of the biotinylated protein and antibody in sera results in a biotinylated protein–antibody complex that is captured simultaneously by the streptavidin-coated donor beads and the protein

A-conjugated acceptor bead. The resultant proximity of the acceptor and donor bead generates the luminescent signal upon irradiation at 680 nm. This is illustrated in Figure 1B.

For biotinylation of the target protein, the N-terminus of the target was fused to the bls, and the cell-free system was supplemented with BirA and biotin.[13] This biotin ligation method yields a biotin labeling on the bls, indicating a specific recognition of the target protein by AlphaScreen. To investigate the specificity and sensitivity of the antibody detection, translation mixtures expressing biotinylated or nonbiotinylated p53 protein were incubated with various concentrations of monoclonal antibody, ranging from 5×10^{-3} to 5×10^{2} pg/μL. This luminescence method specifically detected interaction of monoclonal antibody and the biotinylated p53 from the unpurified translation mixture, whereas nonbiotinylated p53 and biotinylated DHFR did not produce a significant luminescent signal (Figure 1C). In this condition, the biotinylated p53 was detected by anti-p53 antibody at concentrations as low as 0.5 pg/μL. Next, we investigated whether this luminescence method could detect the biotinylated protein–antibody complex in the presence of mouse serum. Translation mixture expressing biotinylated p53 protein was incubated with various concentrations of monoclonal antibody from 2 to 200 pg/μL and mouse immunoglobulin from 0.4 to 40 ng/μL. Figure 1D showed that this method could specifically detect the immunocomplex of biotinylated p53 protein and monoclonal antibody in the presence of an excess of mouse immunoglobulin. In addition, comparison between the specific luminescence and background signals indicated that biotinylated p53 could be detected at more than 0.05% of anti-p53 antibody in mouse serum (Figure 1E). These results indicate that this system is a highly specific and sensitive method for detection of interaction between biotinylated recombinant protein and antibody in whole serum.

Detection of Autoantibodies against Hars and LmnB2 Proteins in sera of MRL/lpr Mice. We next tested our protocol for the well-characterized autoantigens histidyl-tRNA synthetase (Hars)[21] and lamin B2 (LmnB2)[22] in the autoimmune disease model mouse MRL/lpr.[23] To determine the assay conditions using serum samples, biotinylated recombinant Hars and LmnB2 proteins were used (Figure 2A) to detect autoantibody in the sera of MRL/lpr mice. Cell-free synthesis of biotinylated Hars and LmnB2 demonstrated yields of 820 and 600 nM, and 43.0 and 56.4% of biotinylation, indicating biotinylated Hars and LmnB2 proteins were 354.4 and 338.5 nM, respectively. Various volumes (0.003 to 4 μL) of translation mixture expressing biotinylated Hars or LmnB2 protein were incubated with the serum of MRL/lpr mouse (final 1:1000 dilution) in 25 μL of reaction volume (Figure 2B). Significant luminescent signals were observed at additions of biotinylated Hars or LmnB2 proteins between 0.01 and 1 μL, which corresponds to biotinylated protein concentrations between 0.14 and 14 nM or 0.13 and 13 nM, respectively. Also serum dilutions between 1:500 and 1:10 000 produced high luminescence signal in 25 μL of reaction volume using 1 μL of the translation mixtures (Figure 2C). These results mean that five micro litter of serum and 200 μL of cell-free translation mixture expressing biotinylated proteins would be sufficient for 200 assays. Taken together, these results suggest that the luminescence method using cell-free expressed biotinylated proteins would be useful for screening the reaction of autoantigen proteins with autoantibodies in serum.

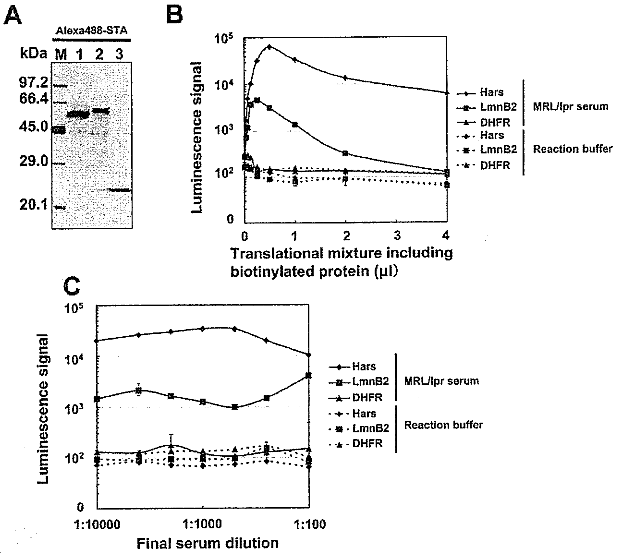

Figure 2. Detection of autoantibodies against Hars and LmnB2 proteins. (A) Biotinylated histidyl-tRNA synthetase (Hars) (lane 1), and lamin B2 (LmnB2) (lane 2) and DHFR (lane 3) proteins were detected by immunoblotting analysis using Alexa488-STA. M indicates protein molecular weight marker. (B) Various volumes (0.003 to 4 μL: representing 2.5–3280 nM Hars, 1.8–2400 nM LmnB2 and 6.4–8520 nM DHFR) of translation mixture expressing biotinylated Hars, LmnB2 or DHFR proteins were incubated with serum of MRL/lpr mouse sera (final 1:1000 dilution) in 25 μL of reaction volume. (C) Serum dilution between 1:100 and 1:10 000 was incubated with 1 μL of the translation mixtures in 25 μL of reaction volume.

Construction of the BPL by the Wheat Cell-Free Protein Production System. It has long been thought that comprehensive screening using a protein library is a strong tool for identification of antigen proteins.[12,24,25] The scheme for the BPL-based screening is shown in Figure 3A. To construct the N-terminal BPL, we selected 226 genes (Supplementary Table 1, Supporting Information) that included well-known autoantigen proteins and proteins coded by genes in the mouse autoimmune susceptibility loci[26] from the mouse full-length cDNA resource (FANTOM).[27,28] For biotinylation, a bls was fused onto 5′ site of a target gene by "split-primer" PCR.[13] Using the PCR, 222 (98.2%) out of 226 genes were successfully amplified and of those, 217 (96%) were transcribed. Synthesis of biotinylated proteins was performed on the GenDecoder1000,[19] and expression confirmed by SDS-PAGE combined with immunoblot analysis using Alexa488-STA (Figure 3B). Finally 214 clones (94.6%) were produced as biotinylated proteins (Supplementary Table 1, Supporting Information) at maximum and minimum concentrations of 500 and 10 nM respectively (data not shown). From our results in Figure 2B, the immunoresponse of biotinylated proteins could be detected below 0.2 nM by the luminescence method, indicating that all 214 proteins are at concentrations viable for screening. Therefore, we used these proteins as the BPL for screening of autoantigen proteins.

BPL-Based Screening of Autoantigen Proteins Using the MRL/lpr Mouse Sera. To identify autoantigen proteins reacting with antibodies in serum of autoimmune disease mice, the BPL and sera from pools of MRL/lpr or normal mouse sera (NMS)

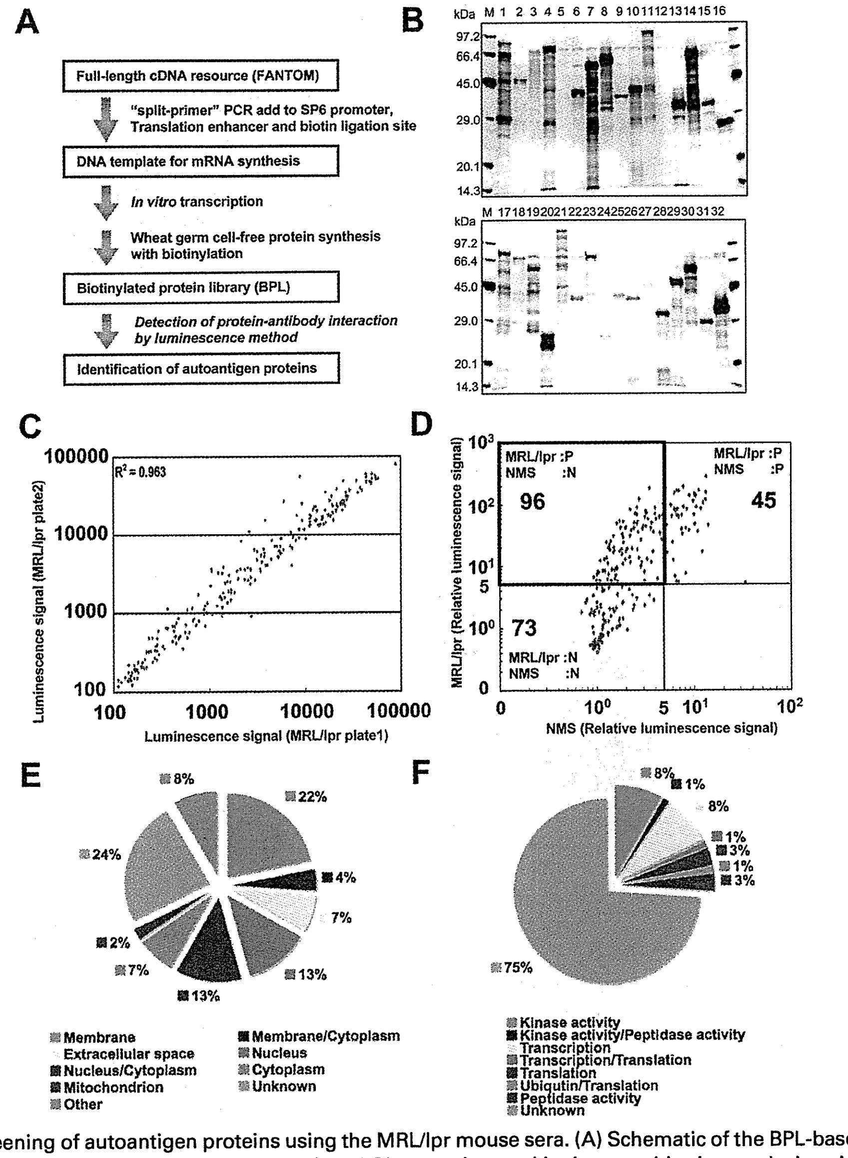

Figure 3. BPL-based screening of autoantigen proteins using the MRL/lpr mouse sera. (A) Schematic of the BPL-based screening method. (B) Thirty-two randomly selected biotinylated proteins of the BPL were detected by immunoblotting analysis using Alexa488-STA. (C) Scatter plot showing the luminescent signals in each well of two independent screening data sets using MRL/lpr mouse sera. The *x*-axis indicates luminescence signals in MRL/lpr plate 1 whereas the *y*-axis represents those in MRL/lpr plate 2. (D) Each data point represents luminescence signals using MRL/lpr mouse sera or normal mouse sera (NMS). The *x*-axis indicates luminescence signals in NMS whereas the *y*-axis represents those in MRL/lpr mice. (E, F) Ninety-six proteins identified as autoantigen proteins were grouped by protein localization in cells (E) Membrane (GO:0016020), Nucleus (GO:0005634), Cytoplasm (GO:0005737), Extracellular region (GO: 0005576) and Mitochondrion (GO:0005739) and biological function/process (F) Kinase activity (GO:0016301), Peptidase activity (GO: 0008233), Ubiquitin (GO:0005551), Translation (GO:0006412) and Transcription (GO:0006350) according to Gene Ontology Database. Minor groups less than 3 proteins were belonged to "Other" group. More detailed information on individual proteins was indicated in the Table 1.

were used. In each well of a 384-well plate, a translation mixture expressing biotinylated protein was incubated with either serum for 30 min, and subsequently a mixture of donor and acceptor beads was added to each well (see Figure 1B). After incubation, antigen–antibody reaction of the BPL was detected by the luminescence assay as described above. As shown in the scatter plot (Figure 3C), the intensity of paired luminescent signals in each well of two independent screening data sets (plate 1 and 2) using MRL/lpr mouse sera showed a linear distribution with a R^2 of 0.963, indicating reproducibly sufficient score for screening. We then compared the luminescent signals of the BPL reacted with MRL/lpr sera and NMS (Figure 3D). In this assay, only 141 of the 214 proteins in the BPL were identified as positive clones, which was indicated by a luminescence signal 5-fold higher than the average background signal. Only 96 proteins in the 141 positive clones reacted with MRL/lpr sera, whereas the remaining 45 proteins interacted with both sera. From these results, 96 proteins were identified as autoantigen proteins in MRL/lpr mice (Table 1, upper left panel in Figure 3D). In these MRL/lpr autoantigen proteins, 25 well-known autoantigens were included, and 71 out of 96 clones were coded in the genetic loci on chromosome 10; 40 cM, chromosome 15; 18 cM and chromosome 19; 49 cM,[26] indicating that this screening identified new MRL/lpr sera

Table 1. List of 96 Identified Proteins As Autoantigen Proteins

gene symbol	source[a]	M_w (kDa)	MRL/lpr[b]	NMS[b]	Gene Ontology[c]: cellular location	Gene Ontology[c]: biological function/process
Agpat3	Chr 10_40	43.3	49.7	2.6	Me	
Bcr	Chr 10_40	35.3	6.4	1.5		K
Unc5b	Chr 10_40	103.7	42.3	3.6	Me	
Pyp	Chr 10_40	33.0	6.3	1.3		
Cdc2a	Chr 10_40	34.1	11.9	3.6	N	K
Cnnm2	Chr 19_49	96.6	64.4	4.4	Me	
Thop1	Chr 10_40	78.0	38.9	2.3	C	K, P
Hhex[d]	Chr 19_49	30.0	54.7	1.9	N	Tc
Palm	Chr 10_40	41.6	59.4	4.1	C, Me	
Gnaz	Chr 10_40	40.8	72.2	5.0	Me	
2610028F08Rik	Chr 15_18	28.3	17.9	1.7		
Ank	Chr 15_18	54.3	55.7	1.7	Me	
Nov	Chr 15_18	38.8	20.4	1.5	E	
Neurl	Chr 19_49	36.0	58.0	4.8		
Gpam	Chr 19_49	93.4	54.2	2.6	Mi, Me	
Ncald	Chr 15_18	22.2	5.9	1.1		
Wnt8b	Chr 19_49	40.5	13.8	2.7	E	
Timp3	Chr 10_40	24.2	19.8	2.3	Me, E	K
Osr2	Chr 15_18	30.6	17.2	1.5	N	
Nnpl	Chr 10_40	54.6	51.3	3.7		
Nfic	Chr 10_40	48.8	80.4	3.2	N	Tc
Pfkl	Chr 10_40	85.4	8.3	3.1	C	K
Slc18a2	Chr 19_49	55.8	72.5	2.5	C, Me	
Sgta[d]	Chr 10_40	34.2	23.0	1.3		
Hps6	Chr 19_49	87.3	59.5	3.4		
Sgpl1	Chr 10_40	63.7	90.9	4.0	Me	
Pdxk	Chr 10_40	35.1	8.1	1.0	C	K
Pwp2h	Chr 10_40	102.9	36.3	2.7		
Psap	Chr 10_40	61.1	42.2	2.4	Mi, E	
Fzd6	Chr 15_18	79.1	92.0	2.6	Me	
Ilvbl	Chr 10_40	68.2	45.8	3.0	Me	
Itgb2	Chr 10_40	84.9	41.7	2.9	Me	
Cstb	Chr 10_40	11.0	18.9	1.4	N, C	
Gstt2	Chr 10_40	27.6	25.1	1.3	N, C	
Bsg	Chr 10_40	29.7	20.4	1.3	Me	
Cpn1	Chr 19_49	52.1	6.1	1.0	E	P
Eif3s6	Chr 15_18	52.0	8.7	1.2		
Timm9	Chr 10_40	10.4	14.2	2.2	Mi, Me	
Ndufs7	Chr 10_40	24.7	11.8	2.9	Mi, Me	
Psd	Chr 19_49	12.4	51.6	2.4	Me	
Tfam	Chr 10_40	28.0	17.8	2.0	N, Mi	Tc
Ppap2c	Chr 10_40	31.2	51.2	1.6	Me	
Gpx4	Chr 10_40	22.1	18.1	1.5	N, C, Mi, Me	
Pcbd1	Chr 10_40	12.0	44.4	2.0	N, C	Tc
Ins1	Chr 19_49	12.2	30.1	1.9	E	
Mrpl54	Chr 10_40	15.4	8.5	1.0	Mi	
Oaz1	Chr 10_40	25.1	11.4	1.3		
Cxxc6	Chr 10_40	25.6	32.1	1.5		
Sdc2	Chr 15_18	22.1	42.5	2.0	Me	
Npm3	Chr 19_49	19.0	13.1	1.2	N	Tc
Eif4ebp2	Chr 10_40	12.9	7.6	1.0	Tl	
Ddt	Chr 10_40	13.1	5.1	0.9	C	
Pah	Chr 10_40	51.8	32.1	2.2		
Peo1	Chr 19_49	77.0	6.8	0.9	Mi	
Cabin1	Chr 10_40	65.2	13.8	1.3	N	
Lilrb4	Chr 10_40	37.5	9.0	1.4	Me	
Casp7	Chr 19_49	34.1	7.6	1.3	C	P
Matk	Chr 10_40	53.6	72.9	4.0	C, Me	K
Egr2	Chr 10_40	49.8	74.7	3.2	N	Tc
Slc1a6[d]	Chr 10_40	60.8	126.0	2.7	Me	
Adn	Chr 10_40	28.1	63.8	3.1		
Gnal1	Chr 10_40	42.0	69.7	4.7		
Tbxa2r	Chr 10_40	37.1	43.9	1.8	Me	
Trhr	Chr 15_18	44.6	188.7	3.5	Me	
Ube2g2	Chr 10_40	33.0	16.0	1.8		U, Tl
Madcam1	Chr 10_40	43.6	33.5	1.8	Me	
Pcdh15	Chr 10_40	129.9	70.6	2.6	C, Me	
Efna2	Chr 10_40	23.6	5.3	1.0	Me	
Sema5a	Chr 15_18	120.3	19.1	1.8	Me	
Aire	Chr 10_40	18.0	8.6	1.2	N, C	Tc, Tl
Fgf8	Chr 19_49	24.7	11.1	1.8	E	
Snrpd2	AA*	13.6	13.4	3.3	N	
Hmgn2	AA	9.4	85.7	2.2	N, C	
Mcrs1	AA	51.7	45.5	3.2	N	
Hnrpa2b1	AA	32.5	19.5	2.1		
Hars	AA	57.4	104.9	4.8	C	Tl
Rpo1−3	AA*	15.1	6.4	4.2		

Table 1. Continued

gene symbol	source[a]	M_w (kDa)	MRL/lpr[b]	NMS[b]	Gene Ontology[c] cellular location	biological function/process
Hars2	AA*	23.4	7.3	1.6	C, Mi	Tl
Hspca	AA	84.8	5.9	3.1		
Vtn	AA	54.8	5.8	1.6	E	
Snrpd3	AA*	13.9	10.2	2.8	N, C	
Hmgn1	AA*	10.1	35.6	4.5	N, C	Tc
Rnps1	AA	40.8	26.0	1.4	N, C	
Fbl	AA	34.2	24.9	1.9	N	
Npm1	AA	32.6	12.6	1.1	N, C	K
Top3b	AA*	96.9	18.9	2.6		
Coil	AA	62.2	9.8	1.6	N	
Casp8	AA	55.4	27.5	2.8	N, C	P
Ybx1	AA	35.7	27.8	4.7	N, C	Tc
Srpk1	AA	73.1	17.7	3.8	N, C	K
Rpa1	AA	71.4	36.6	3.8	N	
Car9	AA*	47.3	8.9	1.5	Me	
Sag	AA	44.9	11.9	2.2		
Dnahc8	AA	122.1	9.2	1.6	C	
Top3a	AA*	107.0	13.1	2.0		
Fbn2	AA	56.6	5.9	1.4	E	

[a] The source of selected gene done by symbol, is as follows: Chr 10_40, genetic loci on chromosome 10_40 cM; Chr 15_18, genetic loci on chromosome 15_18 cM; Chr 19_49, genetic loci on chromosome 19_49 cM; AA, well-known autoantigen; AA*, well-known autoantigen homologue. [b] Relative luminescence signals. [c] According to Gene Ontology (GO) Database (http://www.geneontology.org/), the proteins were classified by cellular localization and biological function/process, is as follows: Me, Membrane (GO:0016020); N, Nucleus (GO:0005634); C, Cytoplasm (GO:0005737); E, Extracellular region (GO:0005576); Mi, Mitochondrion (GO:0005739); K, Kinase activity (GO:0016301); P, Peptidase activity (GO:0008233); U, Ubiquitin (GO:0005551); Tl, Translation (GO:0006412); Tc, Transcription (GO:0006350). [d] Hhex, lane1; Sgta, lane3; Slc1a6, lane4 in Figure 4.

reactive autoantigen proteins. Interestingly, these loci were reported as the susceptibility loci of arthritis. Furthermore, according to Gene Ontology (GO) Database (http://www.geneontology.org/), 73 (76%) of the proteins were classified by cellular localization (Figure 3E) and 25 (26%) classified by biological function/process (Figure 3F). The annotated proteins found were classified as localized with Membrane (22%), Membrane/Cytoplasm (4%), Extracellular space (7%), Nucleus (13%), Nucleus/Cytoplasm (13%), Cytoplasm (7%) and Mitochondrion (2%). Also, the annotated proteins were involved in diverse biological functions/processes such as Kinase activity (8%), Kinase activity/peptidase activity (1%), transcription (8%), Transcription/Translation (1%), Translation (3%), Ubiquitin/Translation (1%) and Peptidase activity (3%). Data analysis showed that 26 and 25 proteins were annotated in localization of nucleus and cytoplasm respectively (Figure 3E, Table 1), and that 9 and 9 proteins were related to cellular events of protein phosphorylation and transcription, respectively (Figure 3F, Table 1). Many nuclear proteins were reported as autoantigens.[2] Interestingly, localization of 38 (39.6%) antigen proteins reacting with antibodies in MRL/lpr mouse sera was annotated in membrane and/or extracellular space. These results suggest that the wheat cell-free system is a viable platform to study folded membrane proteins that function as antigens. The data analysis suggests that MRL/lpr autoantigen proteins are represented by a wide variety of biological functions localized in whole cells, rather than just nuclear proteins. Taken together, these results indicate that the BPL-based screening method would be useful for identification of autoantigen proteins.

Validation of Identified Autoantigen Proteins by Immunoblotting and Immunoprecipitation. Recent reports have mentioned the possibility that autoantibodies may react with conformational epitopes.[29−31] These data were obtained by liquid phase immunoprecipitation assays using recombinant proteins.[32,33] Under these situations, autoantigen proteins we found were analyzed by immunoblotting and immunoprecipitation. For this analysis, six proteins were randomly selected (see legend in Figure 4). Immunoblot analysis showed that three proteins reacted with MRL/lpr mouse sera (Lanes 2, 5, and 6 in Figure 4A). Two of these three proteins, LmnB2 (Lane 5) and topoisomerase II alpha (Top2a) (Lane 6), have been well characterized as autoantigen proteins so far.[22,34] Also, six of our identified autoantigen proteins were not detected by immunoblot analysis in the sera of NMS (data not shown). Interestingly, immunoprecipitation analysis revealed antigenicity of all six autoantigen proteins (Figure 4B, C), whereas two proteins randomly selected from nonautoantigen proteins, serving as a negative control, did not show significant reaction to the sera from MRL/lpr mice by both immunoblot analysis and immunoprecipitation (Lanes 7 and 8 in Figure 4A, B). These results suggest that the BPL-based screening method may be useful for identification of autoantigen proteins reacting with autoantibodies recognizing conformational epitopes.

Discussion

To address high-throughput protein production, we have utilized our wheat germ high-throughput protein synthesis system,[10,16] which can produce large numbers of recombinant proteins using a fully automated robot.[19] To create a library of target autoantigen proteins, full-length human and mouse cDNA resources were provided by the Mammalian Gene Collection (MGC) clones (Mammalian Gene Collection Program, http://mgc.nci.nih.gov/) and FANTOM.[27,28] Since the full-length cDNA was provided in plasmids, no additional time-consuming cloning steps were needed for the synthesis of linear DNA templates by PCR for direct entry into the cell-free based protein production system. Additionally, researchers can select and use any appropriate peptide tag for downstream applications, like a bls used in this study, owing to the ease of template construction. In fact, given the advantages of the gateway system and PCR, a recent publication reported successful production of 13 000 His-tagged human proteins by the wheat cell-free system using full-length cDNA resources.[12] Furthermore, because protein purification is a time-consuming-step, an assay system with no purification requirement could dramatically increase the throughput. For that, a specific

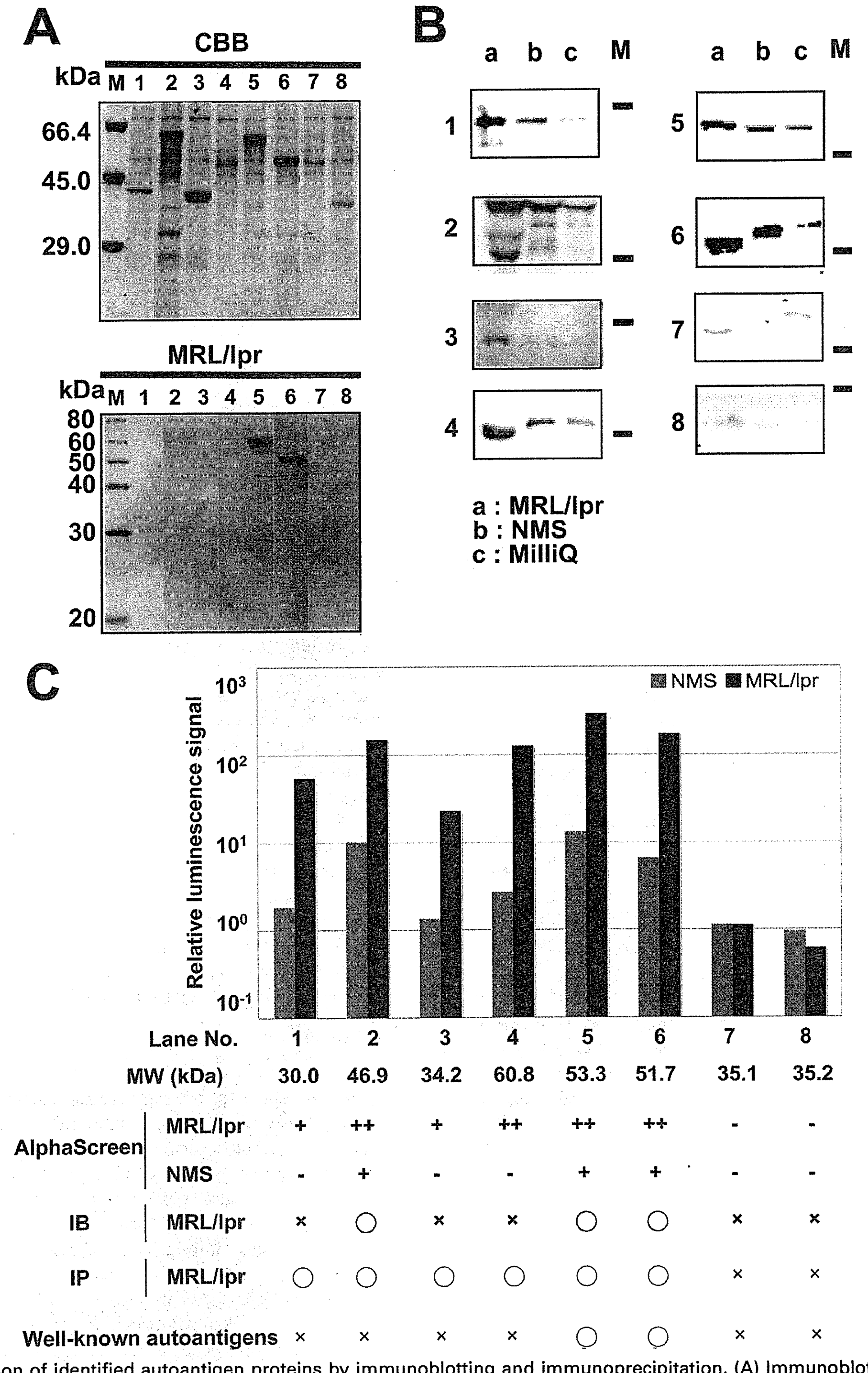

Figure 4. Detection of identified autoantigen proteins by immunoblotting and immunoprecipitation. (A) Immunoblotting analysis by using recombinant proteins. Purified recombinant proteins were separated by SDS-PAGE and stained with CBB (Upper). Purified recombinant proteins were reacted with serum from MRL/lpr mouse (Lower). (B) Immunoprecipitation analysis using recombinant proteins. Translation mixtures expressing biotinylated proteins were incubated with 1 μL of undiluted serum overnight at 4 °C. Immobilized Protein A sepharose was added to each sample, and incubated for 60 min at 4 °C. After washing, proteins were separated by SDS-PAGE, followed by immunoblotting with Alexa488-STA. M indicates a 45 kDa protein molecular weight marker. (C) Whole data of randomly selected proteins. IB, Immunoblotting; IP, Immunoprecipitation. Relative luminescence signal, $10^2 \leq$ ++; $5 \leq + < 10^2$; − < 5. (A, B, C) Lane 1, Hhex; Lane 2, Tdg; Lane 3, Sgta; Lane 4, Slc1a6; Lane 5, Lmnb2; Lane 6, Top2a; Lane 7, Cs; Lane 8, Car4. Lane 7 and 8 were negative controls. Detailed information on individual proteins was indicated in Supplementary Table 1 (Supporting Information).

protein has to be clearly recognized in a homogeneous condition. In this study, we selected biotin as our target protein label due to the highly specific binding of biotin-streptavidin. Commonly, biotinylated proteins are produced via NHS ester-activated biotins. However, this technique requires laborious purification to remove any nonreacted biotin reagent in the reaction mixture. Therefore, we used a BirA biotin-ligase-based labeling system. By addition of BirA and biotin to the wheat cell-free system, highly specific biotin-labeling is available and the biotinylated proteins can be directly used for assaying[13,15,35] without further purification. Taken together, the biotinylated protein library produced by the wheat cell-free system is suitable for autoantigen screening.

Several autoantigen screening methods such as SERPA, SEREX and protein microarray are currently widely used for identification of autoantigen proteins, each of which has inherent limitations. In this study, we demonstrated improved methodologies that overcome the aforementioned limitations using a wheat cell-free based BPL and luminescence assay that allow detection of autoantigen proteins with autoantibodies in sera. The BPL-based screening revealed that specific antibody interaction were detected at subpicogram scale, with a linear response over a 1000-fold range, and appear to be more sensitive than conventional method, such as ELISA.[6,36] It should be noted that protein microarray could also detect autoantigen at picogram scale, in the linear fashion over a 1000-fold range.[6] While the detection sensitivity of the BPL-based autoantigen protein screening method might be equivalent to microarray based autoantigen protein screening, the folded state of the autoantigen proteins differs. The reports which autoantibodies would recognize conformational epitopes[29,30] might contain an important implication for screening of autoantigen proteins. Although conventional methods use denatured or unfolded proteins, such as dehydrated or detergent-treated proteins, the BPL-based method tested in this study better represents the folded, native form as all procedures are carried out in the solution phase without dehydration or detergent treatment. In addition, the BPL-based screening method using serum dilutions of 1:10 000 could produce high luminescent signal in 25 μL of reaction volume (Figure 2C). Thus, 50 μL of serum would be sufficient to screen 20 000 kinds of human proteins.

Autoimmune diseases were thought to be a complex of both genetic and nongenetic factors influencing susceptibility, severity and response to therapies.[37] Twin and family studies suggest that approximately 60% of susceptibility is due to genetic factors and genes within the HLA locus, particularly HLA-DRB1, which accounts for almost half of the genetic component of susceptibility.[37] Also, genetic analyses identified that other susceptibility locus of RA, SLE, and so on.[38] In this study, we screened proteins encoded by genes on an autoimmune susceptibility loci,[26] and 71 out of 111 clones (Table 1 and Supplementary Table 1, Supporting Information) localized on the chromosomes 10, 15 and 19[26] were found as new autoantigen proteins reacting with the sera of MRL/lpr mice. Additionally, the Gene Ontology (GO) Database may be extremely useful for the screening of autoantigen protein. For example, based on data from the GO Database, localization of 38 (39.6%) autoantigen proteins out of 96 MRL/lpr autoantigen proteins were annotated in membrane and/or extracellular space (Figure 3E). These results suggest that a specific protein library focused on the human autoimmune susceptibility loci and membrane proteins or extracellular spaces classified according to GO Database may be a good target for screening of autoantigen proteins.

A key obstacle for robust genome-wide screening has been experimentally simple techniques and automated technology. The BPL-based screening method is one of the simplest approaches for identification of autoantigen proteins, because all experimental processes, including construction of DNA templates, and interaction and detection of antigen−autoantibodies reactions, were reduced to mixing steps. Synthesis of the biotinylated protein library was accomplished using a fully automated robot,[19] and the biotinylated proteins can be used in subsequent screening steps without purification. The method described here can be used in developed for use in 96, 384 (Figure 3A) or 1536-well microtiter-plate format through the use of appropriate automated liquid handling robots. Therefore this method is suitable for development of a genome-wide screening platform. In conclusion, the BPL-based screening method has a high potential for identification of autoantigen proteins in human autoimmune diseases.

Abbreviations: Alexa488-STA, streptavidin Alexa Fluor 488 conjugate; NMS, normal mouse sera; SEREX, serological expression cloning; SERPA, serological proteome analysis; bls, biotin ligation site; DHFR, dihydrofolate reductase; Lmnb2, lamin B2; Hars, histidyl-tRNA synthetase; Top2a, topoisomerase II alpha; Hhex, hematopoietically expressed homeobox; Tdg, thymine DNA glycosylase; Sgta, small glutamine-rich tetratricopeptide repeat (TPR)-containing, alpha; Slc1a6, solute carrier family 1 (high affinity aspartate/glutamate transporter), member 6; Cs, citrate synthase; Car4, carbonic anhydrase 4; BPL, biotinylated protein library; FANTOM, functional annotation of mouse; CBB, coomassie brilliant blue; RF, rheumatoid factor; hnRNP, heterogeneous nuclear ribonucleoprotein; Sm, Smith; GO, Gene Ontology; NHS, *N*-hydroxysuccinimide; RA, rheumatoid arthritis; SLE, systemic lupus erythematosus; MRL/lpr, MRL/Mp-*lpr/lpr*.

Acknowledgment. This work was partially supported by the Special Coordination Funds for Promoting Science and Technology by the Ministry of Education, Culture, Sports, Science and Technology, Japan (T.S. and Y.E.). We thank Michael Andy Goren and Dr. Akira Nozawa for proofreading this manuscript.

Supporting Information Available: Supplementary Table 1: List of selected 226 mouse genes and primer sequences used in this study. This material is available free of charge via the Internet at http://pubs.acs.org.

References

(1) Davidson, A.; Diamond, B. *N. Engl. J. Med.* **2001**, *345* (5), 340–50.
(2) von Mühlen, C.; Tan, E. *Semin. Arthritis Rheum.* **1995**, *24* (5), 323–58.
(3) Mewar, D.; Wilson, A. *Biomed. Pharmacother.* **2006**, *60* (10), 648–55.
(4) Gunawardana, C.; Diamandis, E. *Cancer Lett.* **2007**, *249* (1), 110–9.
(5) Anderson, K.; Ramachandran, N.; Wong, J.; Raphael, J.; Hainsworth, E.; Demirkan, G.; Cramer, D.; Aronzon, D.; Hodi, F.; Harris, L.; et al. *J. Proteome Res.* **2008**, *7* (4), 1490–9.
(6) Robinson, W.; DiGennaro, C.; Hueber, W.; Haab, B.; Kamachi, M.; Dean, E.; Fournel, S.; Fong, D.; Genovese, M.; de Vegvar, H.; et al. *Nat. Med.* **2002**, *8* (3), 295–301.
(7) Hudson, M.; Pozdnyakova, I.; Haines, K.; Mor, G.; Snyder, M. *Proc. Natl. Acad. Sci. U.S.A.* **2007**, *104* (44), 17494–9.
(8) Sheridan, C. *Nat. Biotechnol.* **2005**, *23* (1), 3–4.
(9) Zhu, H.; Snyder, M. *Curr. Opin. Chem. Biol.* **2003**, *7* (1), 55–63.

(10) Sawasaki, T.; Ogasawara, T.; Morishita, R.; Endo, Y. *Proc. Natl. Acad. Sci. U.S.A.* **2002**, *99* (23), 14652–7.
(11) Endo, Y.; Sawasaki, T. *Methods Mol. Biol.* **2005**, *310*, 145–67.
(12) Goshima, N.; Kawamura, Y.; Fukumoto, A.; Miura, A.; Honma, R.; Satoh, R.; Wakamatsu, A.; Yamamoto, J.; Kimura, K.; Nishikawa, T.; et al. *Nat. Methods* **2008**, *5* (12), 1011–7.
(13) Sawasaki, T.; Kamura, N.; Matsunaga, S.; Saeki, M.; Tsuchimochi, M.; Morishita, R.; Endo, Y. *FEBS Lett.* **2008**, *582* (2), 221–8.
(14) Beaudet, L.; Bédard, J.; Breton, B.; Mercuri, R.; Budarf, M. *Genome Res.* **2001**, *11* (4), 600–8.
(15) Takahashi, H.; Nozawa, A.; Seki, M.; Shinozaki, K.; Endo, Y.; Sawasaki, T. *BMC Plant Biol.* **2009**, *9*, 39.
(16) Madin, K.; Sawasaki, T.; Ogasawara, T.; Endo, Y. *Proc. Natl. Acad. Sci. U.S.A.* **2000**, *97* (2), 559–64.
(17) Sawasaki, T.; Morishita, R.; Gouda, M.; Endo, Y. *Methods Mol. Biol.* **2007**, *375*, 95–106.
(18) Sawasaki, T.; Hasegawa, Y.; Tsuchimochi, M.; Kamura, N.; Ogasawara, T.; Kuroita, T.; Endo, Y. *FEBS Lett.* **2002**, *514* (1), 102–5.
(19) Sawasaki, T.; Gouda, M.; Kawasaki, T.; Tsuboi, T.; Tozawa, Y.; Takai, K.; Endo, Y. *Methods Mol. Biol.* **2005**, *310*, 131–44.
(20) Stephen, C.; Helminen, P.; Lane, D. *J. Mol. Biol.* **1995**, *248* (1), 58–78.
(21) Miller, F.; Waite, K.; Biswas, T.; Plotz, P. *Proc. Natl. Acad. Sci. U.S.A.* **1990**, *87* (24), 9933–7.
(22) Brito, J.; Biamonti, G.; Caporali, R.; Montecucco, C. *J. Immunol.* **1994**, *153* (5), 2268–77.
(23) Theofilopoulos, A.; Dixon, F. *Adv. Immunol.* **1985**, *37*, 269–390.
(24) Spirin, A. *Trends Biotechnol.* **2004**, *22* (10), 538–45.
(25) Endo, Y.; Sawasaki, T. *Biotechnol. Adv.* **2003**, *21* (8), 695–713.
(26) Nose, M. *Allergol. Int.* **2007**, *56* (2), 79–86.
(27) Okazaki, Y.; Furuno, M.; Kasukawa, T.; Adachi, J.; Bono, H.; Kondo, S.; Nikaido, I.; Osato, N.; Saito, R.; Suzuki, H.; et al. *Nature* **2002**, *420* (6915), 563–73.
(28) Carninci, P.; Kasukawa, T.; Katayama, S.; Gough, J.; Frith, M.; Maeda, N.; Oyama, R.; Ravasi, T.; Lenhard, B.; Wells, C.; et al. *Science* **2005**, *309* (5740), 1559–63.
(29) Xie, H.; Zhang, B.; Matsumoto, Y.; Li, Q.; Notkins, A.; Lan, M. *J. Immunol.* **1997**, *159* (7), 3662–7.
(30) Tuomi, T.; Rowley, M.; Knowles, W.; Chen, Q.; McAnally, T.; Zimmet, P.; Mackay, I. *Clin. Immunol. Immunopathol.* **1994**, *71* (1), 53–9.
(31) Mackay, I.; Rowley, M. *Autoimmun. Rev.* **2004**, *3* (7–8), 487–92.
(32) Lan, M.; Wasserfall, C.; Maclaren, N.; Notkins, A. *Proc. Natl. Acad. Sci. U.S.A.* **1996**, *93* (13), 6367–70.
(33) Grubin, C.; Daniels, T.; Toivola, B.; Landin-Olsson, M.; Hagopian, W.; Li, L.; Karlsen, A.; Boel, E.; Michelsen, B.; Lernmark, A. *Diabetologia* **1994**, *37* (4), 344–50.
(34) Chang, Y. H.; Shiau, M. Y.; Tsai, S. T.; Lan, M. S. *Biochem. Biophys. Res. Commun.* **2004**, *320* (3), 802–9.
(35) Masaoka, T.; Nishi, M.; Ryo, A.; Endo, Y.; Sawasaki, T. *FEBS Lett.* **2008**, *582* (13), 1795–801.
(36) Quintana, F. J.; Farez, M. F.; Viglietta, V.; Iglesias, A. H.; Merbl, Y.; Izquierdo, G.; Lucas, M.; Basso, A. S.; Khoury, S. J.; Lucchinetti, C. F.; Cohen, I. R.; Weiner, H. L. *Proc. Natl. Acad. Sci. U.S.A.* **2008**, *105* (48), 18889–94.
(37) Wordsworth, P.; Bell, J. *Ann. Rheum. Dis.* **1991**, *50* (6), 343–6.
(38) Cornélis, F.; Fauré, S.; Martinez, M.; Prud'homme, J.; Fritz, P.; Dib, C.; Alves, H.; Barrera, P.; de Vries, N.; Balsa, A.; et al. *Proc. Natl. Acad. Sci. U.S.A.* **1998**, *95* (18), 10746–50.

PR9010553

Biochemical and Biophysical Research Communications 397 (2010) 762–766

Contents lists available at ScienceDirect

Biochemical and Biophysical Research Communications

journal homepage: www.elsevier.com/locate/ybbrc

In vitro dissection revealed that the kinase domain of wheat RNA ligase is physically isolatable from the flanking domains as a non-overlapping domain enzyme

Shin-ichi Makino [a,b,1], Tatsuya Sawasaki [a,b,c], Yaeta Endo [a,b,c], Kazuyuki Takai [a,b,c,*]

[a] *Cell-free Science and Technology Research Center, Ehime University, 3 Bunkyo-cho, Matsuyama, Ehime 790-8577, Japan*
[b] *Venture Business Laboratory, Ehime University, 3 Bunkyo-cho, Matsuyama, Ehime 790-8577, Japan*
[c] *Department of Materials Science and Biotechnology, Graduate School of Science and Engineering, Ehime University, 3 Bunkyo-cho, Matsuyama, Ehime 790-8577, Japan*

ARTICLE INFO

Article history:
Received 31 May 2010
Available online 10 June 2010

Keywords:
Multidomain enzyme
Wheat RNA ligase
Domain structure
Cell-free translation

ABSTRACT

Wheat RNA ligase contains 5′-hydroxyl kinase, 2′,3′-cyclic phosphate 3′-phosphodiesterase, and 5′-phosphate 2′-phosphate-3′-hydroxyl RNA ligase activities in a 110-kDa polypeptide. Taking advantage of a wheat cell-free protein production system, we prepared various fragments containing a part of the enzyme. The method allowed us to check the activities of the fragments rapidly, eliminating the time-consuming cloning and sequencing steps for the expression of the fragment proteins. The results showed that each of the three activities can be assigned to a non-overlapping domain that does not require the presence of the other part(s) of the enzyme for its activity. This contrasts to the case of yeast tRNA ligase, in which the central kinase domain has been suggested to require to be tethered to one of the flanking domains for its activity.

1. Introduction

Multidomain proteins are more widely found in eukaryotes than in prokaryotes [1,2], providing an intriguing aspect of protein evolution. In order to understand the complicated function of a multidomain enzyme, the protein is often dissected into smaller functional pieces. Segregating a domain from the enzyme would prove the functionality of each domain. Smaller proteins are also useful, in general, for three-dimensional structure determination. However, it is not always possible to dissect an enzyme into discrete functional domains in spite of the laborious experiments, which may include a time-consuming step of molecular cloning for production of many different protein fragments. An easier method for assessing the activities of truncated proteins is desired.

Wheat RNA ligase is known as a tri-functional enzyme that catalyzes various RNA-ligation reactions, such as that in tRNA splicing [3] and *in vitro* circularization of uncapped RNA [4]. It has three activities, 5′-hydroxyl kinase (hereafter abbreviated as "kinase" or symbolized by "K"), 2′,3′-cyclic phosphate 3′-phosphodiesterase ("CPD" or "P"), and 5′-phosphate 2′-phosphate-3′-hydroxyl RNA ligase ("ligase" or "L") [5–7]. Another plant RNA ligase from *Arabidopsis* [8] has also been characterized well.

Yeast tRNA ligase [9] also has essentially the same three activities, although it has less than 20% sequence homology with the plant RNA ligases [4,8]. The yeast enzyme has its ligase, kinase, and CPD active sites in this order from the N-terminus to the C-terminus [10]. The border between the ligase and kinase domains has been identified: the ligase domain has its activity when it is physically isolated from the remaining C-terminal fragment, and the C-terminal fragment has its kinase and CPD activities when physically isolated from the ligase domain [10]. It is obvious from sequence comparisons that the plant enzymes also have their ligase, kinase, and CPD active sites in this order from the N-terminus, and the *Arabidopsis* enzyme has been dissected into the ligase and kinase-CPD fusion domains [11,12].

An attempt to locate the border between the kinase and CPD domains of the yeast enzyme was made with complementation tests: some combinations of truncated polypeptide fragments complemented a deletion mutant [10]. However, no autonomously active kinase domain has been isolated in spite of the extensive works, suggesting that the kinase domain needs to be tethered to one of the two flanking domains [10,13]. This raises a question why the fusion to only one of the ligase and CPD domain is sufficient for the kinase activity. It seems possible that the domains assembled into a complex containing all the three domains in the complementation tests, *i.e.*, the domains were not physically

* Corresponding author at: Cell-free Science and Technology Research Center, Ehime University, 3 Bunkyo-cho, Matsuyama, Ehime 790-8577, Japan. Fax: +81 89 927 9941.
E-mail address: takai@eng.ehime-u.ac.jp (K. Takai).
[1] Present address: Center for Eukaryotic Structural Genomics (CESG), Department of Biochemistry, University of Wisconsin-Madison, 445 Henry Mall, Madison, WI 53706, USA.

0006-291X/$ - see front matter © 2010 Elsevier Inc. All rights reserved.
doi:10.1016/j.bbrc.2010.06.030

isolated with each other, even though they were present as separate polypeptides. If that was the case, we have to be careful in concluding that the identified kinase-CPD border is a true border that separates the kinase and CPD functions on the primary structure. In addition, not all that is known about the architecture of yeast tRNA ligase applies to plant RNA ligase, considering the narrower substrate specificity in the yeast enzyme than the plant ones [14] as well as the low sequence homology [4,8]. Therefore, a more extensive analysis of domain organization of plant RNA ligase may deepen the understanding of the mechanism of these eukaryotic RNA ligases and evolution of multidomain enzymes.

In this report, we apply a strategy utilizing cell-free protein synthesis aiming at rapidly segregating functional domains from the multidomain enzyme from wheat. We will discuss on possible interactions among the domains in wheat RNA ligase.

2. Materials and methods

Details in materials and methods are provided in Supplementary materials. The DNA sequences for many different enzyme fragments were prepared by PCR with a cDNA clone for wheat RNA ligase [4] as a template [15]. They were transcribed and translated in a wheat-germ cell-free translation system, and the products were purified and qualitatively assayed for the enzyme activities. The sequences for the protein fragments corresponding to the domains identified in this paper were subcloned into a cell-free expression vector pEU for large scale cell-free protein production. mRNA preparation and cell-free translation were performed essentially according to the previous paper [15] with some optimization. Enzyme activities were measured using RNA molecules with definite nucleotide sequences and terminal phosphate forms in a buffer containing 20 mM HEPES-KOH (pH 7.8), 250 mM NaCl, 80 mM potassium acetate, 2 mM magnesium acetate, 2 mM DTT, 0.01% (w/v) BSA, and 1 mM ATP when required.

3. Results

3.1. Construction of enzyme fragments and separation of the three activities

In order to locate the three functional domains of the wheat RNA ligase enzyme on its primary structure, we constructed various protein fragments as listed in Fig. 1. Each enzyme fragment was synthesized as an N-terminal GST-fusion by the wheat cell-free translation system without cloning into a plasmid (Fig. S1 in Supplementary materials). Initially we constructed a series of N-terminal and C-terminal truncations. The C-terminal 613-1042 fragment had the kinase and CPD activities. Those activities were detected by a shift in the electrophoretic mobility of an RNA molecule (Fig. S2) and were confirmed by measuring the change in the molecular mass by TOF-MS analyses. This fragment was useful for producing an RNA substrate with the 5′-phosphate and 3′-hydroxyl-2′-phosphate termini, which was used for the detection of the core ligase activity. The remaining N-terminal 1-612 fragment had the core ligase activity. This is consistent with the previous data on yeast and *Arabidopsis* enzymes [11]. The 1-612 and 613-1042 fragments are symbolized in this paper by L and KP, respectively.

In order to dissect the two end-modifying activities of the C-terminal half, we applied the same truncation strategy on KP. As a re-

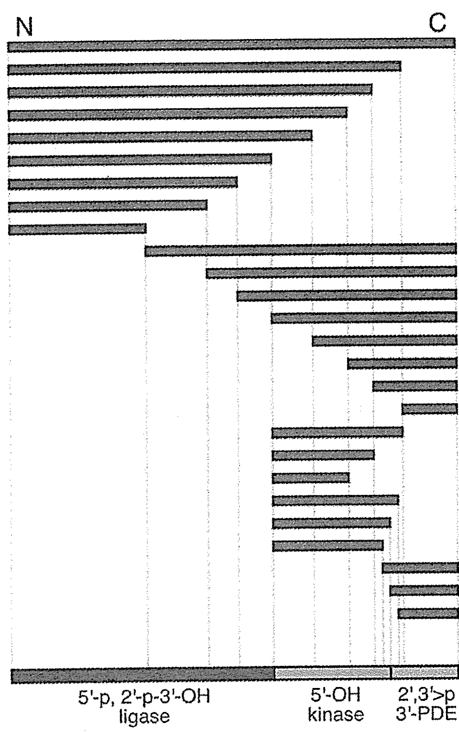

	5'-OH, 2',3'>p ligase	5'-p, 2'-p, 3'-OH ligase	5'-OH kinase	2',3'>p 3'-PDE
1-1042	+	+	+	+
1-915	−	+	+	−
1-848	−	+	−	−
1-790	−	+	−	−
1-708	−	+	−	−
1-612	−	+	−	−
1-532	−	−	−	−
1-462	−	−	−	−
1-320	−	−	−	−
321-1042	−	−	+	+
463-1042	−	−	+	+
533-1042	−	−	+	+
613-1042	−	−	+	+
709-1042	−	−	−	+
791-1042	−	−	−	+
849-1042	−	−	−	+
916-1042	−	−	−	−
613-915	−	−	+	−
613-848	−	−	−	−
613-790	−	−	−	−
613-903	−	−	+	−
613-885	−	−	+	−
613-868	−	−	−	−
869-1042	−	−	−	+
886-1042	−	−	−	+
904-1042	−	−	−	−

Fig. 1. Enzyme fragments generated from the wheat RNA ligase gene and its activity. A schematic diagram shows each location of the fragments containing a part of the enzyme. Fragments are denoted on the right as a combination of the first and the last residue number from the N-terminus of the full-length enzyme. *In vitro* enzymatic activities of each fragment by purified enzymes shown in Fig. S1 are summarized on the right. The domain organization deduced from the activities is shown on the bottom bar.

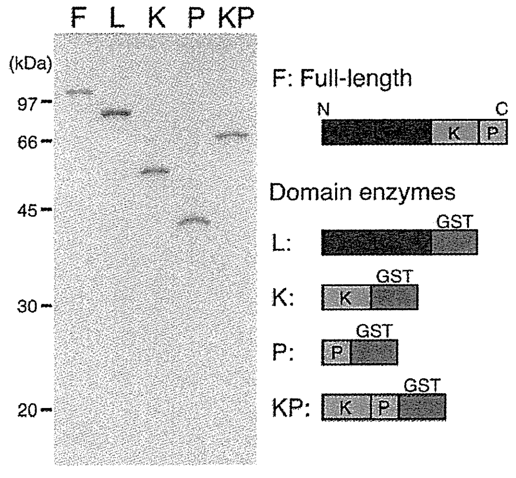

Fig. 2. Proteins used for the biochemical assays. (left panel) An SDS-PAGE image of the domain proteins, with the positions of the size markers indicated on the left. 0.2 μg of each protein was loaded. The gel was stained with CBB. (right panel) Schematic representation of the proteins consisting of the ligase (L), kinase (K), phosphodiesterase (P) domains, and the GST moiety.

sult, we located the CPD activity on the 886-1042 fragment (P), and the kinase activity on the 613-885 fragment (K) (Figs. S1 and S2).

3.2. Synthesis of the domain enzymes

We constructed the plasmids for cell-free expression of the individual functional domains described above as C-terminal GST-fusions. Each protein was successfully synthesized and purified (Fig. 2). These enzymes may be denoted in this paper by the fragment symbols as in the figure. The yields of the purified proteins were 0.88 mg/ml reaction (60 h) for L, 0.18 mg/ml reaction (36 h) for K, 0.66 mg/ml reaction (36 h) for P, and 0.45 mg/ml reaction (36 h) for KP. Each domain enzyme showed the same property as the respective N-terminal GST-fusion in the qualitative assays (data not shown). We also produced the full-length enzyme (F) in the same manner with the yield of 0.031 mg/ml reaction (36 h).

3.3. Comparisons of activities between the full-length enzyme and the domain enzymes

We then characterized the catalytic activities of the domain enzymes as compared with the full-length enzyme. The ligase activities (Fig. 3A and B) were measured by monitoring the product of the intermolecular ligation between two RNAs of defined sequences with the controlled terminal structures shown in Fig. 3A. The F enzyme showed a lag in the ligation reaction between the 5′-hydroxyl and 2′,3′-cyclic phosphate ends, but not between the 5′-phosphate and 3′-hydroxyl-2′-phosphate ends (Fig. 3B). The L domain enzyme had a comparable specific activity to the F enzyme with 80% of substrate RNAs ligated with the equimolar donor/acceptor ratio. Surprisingly, the other domain enzymes had higher specific activities than those of the respective activities of the F enzyme (Fig. 3C and D). We observed an extra band close to that of the 5′-triphosphate RNA in Fig. 3A (center and right), on which we will report elsewhere.

4. Discussion

The present method for mapping functional domains on primary structures of multifunctional proteins through preparation of protein fragments is advantageous over other methods in that it does not include time intensive cloning steps for each truncated construct. Preparation of protein fragments, in general, may suffer from difficulties because some incomplete parts of a domain may cause misfolding of another domain. The use of the wheat cell-free system may also have an advantage in this point, because it seems to have a higher ability to prevent inter-domain misfolding of multidomain proteins than a bacterial system, resulting in a high success rate in soluble protein production [16,17]. Moreover, we noticed another advantage of the wheat cell-free system by the fact that purified enzyme fragments as well as the domain enzymes showed little contamination of ribonucleases so that we were able to check the activity on RNA substrates.

It has been concluded that the kinase domain of yeast tRNA ligase requires to be tethered to at least one of the remaining two flanking domains. *Arabidopsis* RNA ligase has also been separated into an active ligase domain and an active kinase-CPD fusion domain, while it has not been tested if the latter domain can be separated into autonomously active kinase and CPD domains. Our data in Figs. 1 and 3 clearly show for the first time that plant RNA ligase has an autonomous and fully active kinase domain that does not overlap or depend on either the ligase or the CPD domain. In other words, the kinase domain enzyme is physically isolatable from the other two domains: it does not require the presence of either of the two domains for its kinase activity. The boundary between the kinase and CPD domains seems consistent with the previously reported one in yeast tRNA ligase [10]. Therefore, it might be possible that the yeast enzyme can also be dissected into the three isolatable enzymes. The domain activity might be affected by the method for preparation of the protein fragment and even by a single amino acid residue near the boundary of the fragments. On the other hand, our results might also be suggesting that plant RNA ligase is different from yeast tRNA ligase in the tertiary assembly of the domains to form the full-length enzyme. It is an enchanting hypothesis that the difference in the substrate specificity between the yeast and plant enzymes might reflect some difference in the three-dimensional spatial assembly of the domains [14]. It may be possible that selection pressures for the narrower substrate specificity for tRNA and the smaller size in the yeast enzyme have reduced the independence of the kinase domain from the other domains during molecular evolution. More intensive analyses on the yeast enzyme may be required for clearly solving this issue. Some bacteria and a baculovirus have related multifunctional enzymes, while they have a 2′,3′-phosphatase activity instead of the CPD activity [18,19]. For none of these enzymes, the 5′ and 3′ end-modifying activities have been separated physically on the primary structure. T4 polynucleotide kinase, which is considered to provide a 5′-kinase and a 2′,3′-phosphatase activities for T4 RNA ligase, is a homotetrameric protein [20] and is likely to be quite different from the kinase-CPD domain of the yeast and plant RNA ligases.

The time course experiments in Fig. 3 suggest that each domain enzyme is no less active than the corresponding domain in the full-length enzyme. Rather, it seems that the activities of the K and P domain enzymes are higher than the corresponding activities of the KP and F enzymes. It is thus likely that the interaction between the K and P domains suppresses the activity of each domain. We have also noticed that the presence of the tethered L domain seems to inhibit the kinase activity weakly. Nandakumar et al. [11] have reported that the ligase domain enzyme of *Arabidopsis* RNA ligase show substantial suppression on the activities of its kinase-CPD enzyme. While they deduced that the inhibition is due to the high affinity of the ligase domain to RNA substrates according to the report, it may be possible that the native full-length enzyme has suppressive interactions among the domains.

Native assembly of the domains composing a multidomain enzyme may, in general, be intuitively expected to provide a synergistic effect on its activity. By contrast, our proper dissection